

**Dynamical quark mass generation in a strong external magnetic field**Niklas Mueller,<sup>1,2</sup> Jacqueline A. Bonnet,<sup>1</sup> and Christian S. Fischer<sup>1</sup><sup>1</sup>*Institut für Theoretische Physik, Universität Giessen, 35392 Giessen, Germany*<sup>2</sup>*Institut für Theoretische Physik, Universität Heidelberg, 69120 Heidelberg, Germany*

(Received 10 February 2014; published 27 May 2014)

We investigate the effect of a strong magnetic field on dynamical chiral symmetry breaking in quenched and unquenched QCD. To this end we apply the Ritus formalism to the coupled set of (truncated) Dyson-Schwinger equations for the quark and gluon propagator under the presence of an external constant Abelian magnetic field. We work with an approximation that is trustworthy for large fields  $eH > \Lambda_{\text{QCD}}^2$  but is not restricted to the lowest Landau level. We confirm the linear rise of the quark condensate with a large external field previously found in other studies and observe the transition to the asymptotic power law at extremely large fields. We furthermore quantify the validity of the lowest Landau level approximation and find substantial quantitative differences to the full calculation even at very large fields. We discuss unquenching effects in the strong field propagators, condensate and the magnetic polarization of the vacuum. We find a significant weakening of magnetic catalysis caused by the backreaction of quarks on the Yang-Mills sector. Our results support explanations of the inverse magnetic catalysis found in recent lattice studies due to unquenching effects.

DOI: [10.1103/PhysRevD.89.094023](https://doi.org/10.1103/PhysRevD.89.094023)

PACS numbers: 12.38.Aw, 11.30.Rd, 12.38.Lg

**I. INTRODUCTION**

The study of the influence of Abelian background magnetic fields onto the fundamental properties of QCD, confinement and dynamical chiral symmetry breaking is a topic of ever growing interest. Strong time-dependent magnetic fields may play an important role in the early universe and in the initial stages of heavy ion collisions as well as in the interior of dense neutron stars. Magnetic fields influence the thermodynamics of QCD, thereby adding an additional dimension to the phase diagram and presumably changing the phases of matter found in the latter. From a purely theoretical point of view, by tuning an external magnetic field and studying the reaction of QCD, one obtains important insights into the structure of strongly interacting matter, see e.g. [1–4] and references therein.

The influence of magnetic fields onto strongly interacting systems has been investigated in many approaches in the past years. Model calculations involved the quark-meson and Nambu-Jona-Lasinio models, see e.g. [2,5,6]. The functional renormalization group has been invoked to quantify the effects of fluctuations beyond the mean field level [7–10] and lattice gauge theory delivered interesting results at zero and finite temperature [11–20].

With respect to chiral symmetry breaking, an important property of fermionic systems has been pointed out in Ref. [21]. *Magnetic catalysis* describes the effect that a nonvanishing external magnetic field induces a dynamically generated fermion mass, even if the generic interaction strength of the fermionic theory is so small that the system is chirally symmetric otherwise. It is currently debated whether this effect persists or is replaced by *inverse magnetic catalysis* at temperatures around and above the chiral

crossover of QCD [11–13,20,22]. Under debate is also the issue of potential condensation of vector mesons in a strong magnetic field, see [23–25] and Refs. therein. Moreover, the reaction of the electric charges of the quarks inside hadrons to a magnetic field can be used to probe the corresponding color forces. This is the underlying physical idea behind the recently proposed dual Wilson loop [26].

In this work, we employ a functional approach to continuum QCD using Dyson-Schwinger equations (DSEs) to study the influence of magnetic fields onto the quark propagation and the chiral condensate [27–33]. While our long-term goal is to describe the phase diagram of QCD under influence of the magnetic field, in the following, we restrict ourselves to zero temperature and chemical potential. We start out with the quenched theory, using the full Ritus eigenfunction formalism suitable for strong external fields. In this respect, our study is complementary to Ref. [33], where results for the limit of small fields have been discussed. We describe the corresponding formalism in some detail in Sec. II and present results for the quenched theory in Sec. III. We then provide the formalism for the treatment of the unquenched theory in Sec. IV and discuss results for the gluon and quark propagators, the condensate and the magnetic polarization of the vacuum in Sec. V. We summarize our conclusions in Sec. VI.

**II. CONTINUUM QCD IN AN EXTERNAL MAGNETIC FIELD****A. Fermion eigenfunctions in an Abelian background field**

There are different ways of treating a quantum field theory in an external  $U(1)$  field. One is to introduce sources

to which the charged fields of the theory can couple. This makes particular sense if the Abelian field is weak enough to be treated perturbatively and if it vanishes asymptotically. There are, however, interesting systems with strong magnetic fields like neutron stars or heavy ion collisions, where the effects of the magnetic fields must be included to all orders. Furthermore, magnetically noninteracting asymptotic states can only be constructed in special cases, as for example for a field that covers only a finite volume. For very strong fields, one also has to take into account the breaking of Poincaré invariance, rendering the well-known expansion in Fourier modes in a perturbative attempt useless.

The case of a strong external magnetic field is quasi-classical and one can treat the interaction of the charges with the background Abelian field statistically by solving the equations of motion. The resulting eigenfunctions can be used for expansions within the field theory in which one is interested. The advantages of such a procedure are obvious: by transforming into the eigensystem of the particle in the background field, one obtains equations of motion which include the background field, but are formally equivalent to the one of a free particle, see Eq. (1) below. This leads to a set of new Feynman rules that include the interaction with the external field to every order. In order to make the paper self-contained, we summarize this procedure in the following.

One begins with the Dirac equation of a fermion in an arbitrary external  $U(1)$ -valued gauge field

$$(i\gamma \cdot \Pi + m)\Psi(x) = 0, \quad (1)$$

where  $\Pi_\mu = \partial_\mu + ieA_\mu(x)$  is the covariant derivative with electric charge  $e$ . Without loss of generality, this charge can be set to one. For simplicity, let us consider  $A_\mu(x) = (0, 0, Hx, 0)$  corresponding to a constant magnetic field along the  $z$ -direction. It was shown by Ritus [34,35] that the fermion two-point Green's function can only depend on four independent Lorentz scalar structures

$$\gamma\Pi, \quad \sigma F, \quad (F\Pi)^2, \quad \gamma^5 FF^*, \quad (2)$$

with indices omitted that are being summed over. Hereby,  $F$  is the field strength tensor of the magnetic field,  $F^*$  is its dual and  $\sigma^{\mu\nu} = -i/2[\gamma^\mu, \gamma^\nu]$ . All the operators in Eq. (2) commute with  $(\gamma\Pi)^2 = \Pi^2 - \frac{1}{2}e\sigma F$ , thus one is left with solving the eigenvalue equation

$$(\gamma\Pi)^2 E_p = p^2 E_p \quad (3)$$

with the generic eigenvalue  $p^2$  to be determined. Other operators commuting with  $\gamma\Pi$  are  $i\partial_0$ ,  $i\partial_3$  and  $i\partial_2$ , corresponding to the eigenvalues  $p_{\parallel} = (p_0, p_3)$  and  $p_2$ . Thus, the eigenfunctions in the 0, 2- and 3-direction are still

plane waves, whereas the 1-direction resembles a harmonic oscillator.

There is still one further operator, denoted by

$$\mathcal{H} = -(\gamma\Pi)^2 + \Pi_0^2 = \Pi_1^2 + \Pi_2^2 - eH\Sigma^3, \quad (4)$$

that has the same eigenfunctions as the ones in Eq. (2). Here,  $\Sigma^3$  is the third Pauli spin matrix given by  $\Sigma^3 = \sigma^{12}$ . Furthermore,  $\mathcal{H}E_p = kE_p$  and the eigenfunctions  $E_p$  are of the form

$$E_p = E_{p,\sigma}\Delta(\sigma), \quad (5)$$

where  $\Delta(\sigma) = \frac{1}{2}(1 + \sigma\Sigma^3)$  is the spin projector along the  $z$ -axis with the eigenvalues  $\sigma = \pm 1$ . With the above knowledge, the eigenfunctions can be written as

$$E_{p,\sigma} = N_\sigma e^{i(p_0x_0 - p_2x_2 - p_3x_3)} F_{k,p_2,\sigma}. \quad (6)$$

Here,  $F_{k,p_2,\sigma}$  is an unknown scalar function and  $N_\sigma$  a generic normalization. This ansatz can be plugged into Eq. (3) and solved. An instructive derivation can be found in Ref. [32]. One obtains

$$E_{p,\sigma}(x) = N(n) e^{i(p_0x_0 - p_2x_2 - p_3x_3)} D_n(\rho),$$

$$\rho = \sqrt{2|eH|} \left( x_1 - \frac{p_2}{eH} \right), \quad N(n) = \frac{(4\pi|eH|)^{\frac{1}{4}}}{\sqrt{n!}},$$

where  $D_n(\rho)$  are the parabolic cylinder functions, which can be expressed in terms of Hermite polynomials

$$D_n(x) = 2^{-n/2} e^{-x^2/4} H_n(x/\sqrt{2}) \quad (7)$$

of order  $n = l + \frac{\sigma}{2} \text{sgn}(eH) - \frac{1}{2}$ , where the positive integer  $l$  labels the Landau level. Furthermore, between the eigenvalues one finds the relation

$$p^2 = p_0^2 - p_3^2 - k, \quad k = |eH|(2n + 1) + \sigma|eH|, \quad (8)$$

and realizes that  $n$  are the eigenvalues of a harmonic oscillator with  $n \in \mathbb{N}_0$ . In fact,  $l$  is the total angular momentum quantum for each Landau level, realized by two spin directions. Except for the lowest eigenvalue (the lowest Landau level), every fermionic energy value is degenerate with respect to two spin orientations differing by  $\pm 1$ . Furthermore, the transition between two adjacent energy levels (note that these are fermionic eigenstates) is identical to a bosonic spin one transition of a harmonic oscillator. One can regroup the eigenvalues  $n$  and  $\sigma$  and replace them by the quantum number  $l \in \mathbb{N}_0$  in order to label states of different energy. This regrouping is shown exemplarily for the first few Landau levels in the following table. The eigenvalue  $\sqrt{k}$  can be replaced by  $p_{\perp} = \sqrt{2|eH|}l$ , which has the dimension of momentum. The complete set of eigenvalues corresponding to the Ritus

eigenfunctions is  $(p_0, p_3, p_2, l)$  or equivalently the “pseudomomenta”  $(p_0, 0, p_\perp, p_3)$ . Effectively, the magnetic field reduces the problem to  $2 + 1$  dimensions, breaking the Euclidean  $O(4)$  symmetry to an  $O_\parallel(2) \otimes O_\perp(2)$ . The  $O_\perp(2)$  symmetry represents the gauge freedom, for one could have chosen a different vector potential giving the same magnetic field (but a different definition of  $p_\perp$ ). For  $l = 0$  we have  $p_\perp = 0$ , so that the problem is in fact  $1 + 1$  dimensional on the lowest Landau level (LLL).

$l$	$p_\perp = \sqrt{2 eH l}$	$\sqrt{k} = \sqrt{ eH (2n+1) + \sigma eH }$
0	0	$\{n = 0 \sigma = -1$
1	$\sqrt{2 eH }$	$\left\{ \begin{array}{l} n = 0 \quad \sigma = +1 \\ n = 1 \quad \sigma = -1 \end{array} \right.$
2	$\sqrt{4 eH }$	$\left\{ \begin{array}{l} n = 1 \quad \sigma = +1 \\ n = 2 \quad \sigma = -1 \end{array} \right.$
$\vdots$	$\vdots$	$\vdots$

It has been shown that the resulting Ritus basis is orthonormal and complete [27,29],

$$\int d^4x \bar{E}_p(x) E_{p'}(x) = (2\pi)^4 \delta^{(4)}(p - p') \Pi(l) \quad (9)$$

$$\int \frac{d^4p}{(2\pi)^4} E_p(x) \bar{E}_p(y) = (2\pi)^4 \delta^{(4)}(x - y), \quad (10)$$

$$\text{with } \int \frac{d^4p}{(2\pi)^4} = \sum_{l=0}^{\infty} \int \frac{d^2p_\perp}{(2\pi)^4} \int_{-\infty}^{\infty} dp_2$$

and

$$\Pi(l) = \begin{cases} \Delta(\text{sgn}(eH)) & l = 0 \\ 1 & l > 0. \end{cases} \quad (11)$$

Let us further discuss the properties of an expansion in such eigenfunctions. First, by construction, the equations of motion for a fermion in the Ritus basis are formally identical with that of a free particle. Hence, they can be used to add a quantum theory, such as QCD, on top. The Dirac propagator and the fermion self-energy are diagonal in this basis, thus also the self-energy  $\Sigma(x, x')$  satisfies an eigenvalue equation with eigenvalue  $\Sigma(p)$

$$\int d^4x' \Sigma(x, x') E_p(x') = E_p(x) \Sigma(p). \quad (12)$$

There is, however, also a technical difficulty that comes with this method. Since neutral particles such as photons and gluons still have plane waves as eigenfunctions, complications arise whenever they couple to charged particles. Coupling particles that live in different eigenspaces renders the form of the vertex in (pseudo)momentum space complicated, as shall be seen below. As a result, momentum conservation at those vertices is not what one is

used to from covariant field theory. Whereas physical momentum is not conserved, because of the loss of translational invariance caused by the external field, the pseudomomentum Ritus eigenvalues  $(p_0, p_3, p_2, l)$  are conserved along every fermion line.

In the following section, we will derive the Dyson-Schwinger equation for the quark propagator in Ritus functions. We will not be concerned too much with the distinction between momentum and pseudomomentum, for particles will always be expanded in their eigenbasis and it should be clear from the context which eigenvalue is referred to.

## B. Quark Dyson-Schwinger equation in a background magnetic field

In order to write down the quark DSE, we need to expand the fermion fields in terms of Ritus eigenfunctions instead of the usual plane wave Fourier representation as discussed above. The gluon fields do not couple to the magnetic background field and are still to be expanded in plane waves. This is similar with or without quark back-coupling effects to the Yang-Mills sector of the theory, since quarks appear in closed loops only. Thus, the fully dressed gluon remains diagonal in Fourier space. However, in the unquenched theory, the gluons feel the magnetic field due to the modification of the vacuum, filled by charged quark-antiquark pairs. The resulting splitting of the gluon propagator in longitudinal and transverse pieces (with respect to the magnetic field) will be discussed later in Sec. IV. In this section we will treat the quenched case, where the gluon remains isotropic.

Because of these two eigensystems involved, the DSE in a background magnetic field needs a systematic investigation. We will therefore follow [27,29] and start from the DSE in position space in order to derive the equation in (pseudo)momentum space from first principles. This leads to a set of modified Feynman rules describing a quantum theory in a background magnetic field, with the background treated statistically and to every order implicitly already in the propagators and vertices of the theory. The magnetic field is considered as constant and, for convenience, directed along the z-axis, with  $A_\mu = (0, 0, Hx, 0)$  as before. In principle, also nonconstant arbitrary fields can be treated within this method, provided one is able to solve for the eigenfunctions. One example, where the Ritus eigenfunctions can be found analytically, is an exponentially decaying magnetic field, discussed in Ref. [32].

The Dyson-Schwinger equation in position space and with local interaction is given by

$$S^{-1}(x, y) = S_0^{-1}(x, y) + \Sigma(x, y), \quad (13)$$

where the quark self-energy reads

$$\Sigma(x, y) = ig^2 C_F \gamma^\mu S(x, y) \Gamma^\nu(y) D_{\mu\nu}(x, y), \quad (14)$$

with  $C_F \delta_{ij} = (T^a T^a)_{ij}$ , and  $T$  the  $SU(3)$  generators in the fundamental representation. Color indices are omitted in the following. One can now expand this equation in terms of Ritus eigenfunctions. By multiplying with  $\bar{E}_p(x)$  from the left and  $E_{p'}(y)$  from the right (where  $p$  and  $p'$  denote the incoming and outgoing pseudomomenta) the integration over  $x$  and  $y$  yields

$$\begin{aligned} & \int d^4x d^4y \bar{E}_p(x) S^{-1}(x, y) E_{p'}(y) \\ &= \int d^4x d^4y \bar{E}_p(x) S_0^{-1}(x, y) E_{p'}(y) \\ &+ \int d^4x d^4y \bar{E}_p(x) \Sigma(x, y) E_{p'}(y). \end{aligned} \quad (15)$$

Using the completeness relation Eq. (10) one obtains

$$\begin{aligned} & (2\pi)^4 \delta^{(4)}(p - p') \Pi(l) [A_{\parallel}(p) i\gamma p_{\parallel} + A_{\perp}(p) i\gamma p_{\perp} + B(p)] \\ &= (2\pi)^4 \delta^{(4)}(p - p') \Pi(l) [\gamma p + m] + \Sigma(p, p'), \end{aligned} \quad (16)$$

where  $A_{\parallel}(p)$ ,  $A_{\perp}(p)$  and  $B(p)$  are vector and scalar dressing functions of the quark propagator in (pseudo) momentum space, whereas  $\Sigma(p, p')$  denotes the self-energy. The momentum vectors parallel and perpendicular to the magnetic field direction are denoted by  $p_{\parallel} = (p_0, 0, 0, p_3)^T$  and  $p_{\perp} = (0, 0, p_2, 0)^T$ . The self-energy term is implicitly proportional to  $\delta^{(4)}(p - p') \Pi(l)$ , a property that will later also show up explicitly. The DSE for the quark self-energy in the Ritus eigenbasis is then given by

$$\begin{aligned} \Sigma(p, p') &= g^2 C_F \int d^4x d^4y \bar{E}_p(x) \gamma^{\mu} S(x, y) \\ &\times \Gamma^{\nu}(y) D_{\mu\nu}(x, y) E_{p'}(y). \end{aligned} \quad (17)$$

To evaluate this expression, it is necessary to use the representation of the fermion propagator in Ritus eigenfunctions. The eigenvalues of the fermion in an external magnetic field in the configuration given above are  $(p_0, p_3, p_2, l)$  where  $l$  labels the Landau level. The quantum number  $p_2$  is still a ‘‘good’’ (referring to the Fourier eigenfunction) quantum number. However, as seen from the previous section, the energy of the fermion is degenerate with respect to this eigenvalue. The momentum  $p_2$

merely fixes the origin of the  $x_1$  component of our quantum harmonic oscillator system. The momenta of the fermions are  $p_{\parallel}$  and  $p_{\perp}$  or  $(p_0, \sqrt{2|eH|}l, 0, p_3)$ . The fermion propagator in Ritus representation is given by

$$\begin{aligned} S(x, y) &= \int \frac{d^4q}{(2\pi)^4} E_q(x) \\ &\times \frac{1}{i\gamma \cdot q_{\parallel} A_{\parallel}(q) + i\gamma \cdot q_{\perp} A_{\perp}(q) + B(q)} \bar{E}_q(y), \end{aligned} \quad (18)$$

where the sum/integral is over the eigenvalues  $(p_0, p_3, p_2, l)$  as given in Eq. (10). The integration over  $p_2$  accounts for the degeneracy of states of one Landau level. Before proceeding, one should notice that the form of Eq. (18) is used here in analogy to the vacuum case, accounting for the anisotropy by introducing separate dressing functions for the transverse and longitudinal components. In principle, due to the appearance of further Lorenz structures ( $\propto F_{\mu\nu}$ ), the fermion propagator could possess a richer tensor structure. However, as argued in Ref. [29], any other spin dependent tensor structures violate a remaining  $Z(2)$  symmetry of the system by rendering the position of a putative pole structure in the quark propagator dependent on the direction of the external field. In our numerical investigation of the system, we find support for this point of view. When we take into account the additional structures, we obtain nontrivial solutions for  $A_{\parallel}(p)$ ,  $A_{\perp}(p)$ ,  $B(p)$  only together with zero dressing functions in these additional structures. For brevity, we therefore omit these structures here and in the following from the start.

The isotropic Fourier representation of the Landau gauge gluon, as it is used in the quenched approximation, is given by

$$D_{\mu\nu}(x, y) = \int \frac{d^4k}{(2\pi)^4} e^{ik(x-y)} D(k^2) P_{\mu\nu}, \quad (19)$$

where the integration is a momentum integration in the conventional sense since the gluon is still diagonal in Fourier space. The gluon propagator function  $D(k^2)$  is related to the dressing function  $Z(k^2)$  via  $D(k^2) = Z(k^2)/k^2$  and  $P_{\mu\nu} = \delta_{\mu\nu} - k_{\mu}k_{\nu}/k^2$  is the transverse projector. By plugging Eq. (18) and Eq. (19) into Eq. (17), one obtains

$$\begin{aligned} \Sigma(p, p') &= g^2 C_F \int \frac{d^4q}{(2\pi)^4} \int \frac{d^4k}{(2\pi)^4} \int d^4x d^4y \\ &\times \left\{ \bar{E}_p(x) \gamma^{\mu} E_q(x) \frac{1}{A_{\parallel}(q) i\gamma \cdot q_{\parallel} + A_{\perp}(q) i\gamma \cdot q_{\perp} + B(q)} \bar{E}_q(y) \Gamma^{\nu} E_{p'}(y) e^{ik(x-y)} D(k^2) P_{\mu\nu} \right\}. \end{aligned}$$

The quenched gluon propagator  $D(k^2)$  is very well known, both from lattice calculations and solutions of the corresponding DSEs (without background magnetic field) [36–41]. In order to facilitate our later treatment of the unquenched gluon DSE, we use the lattice results of [42] as input for our study. The dressed quark-gluon vertex is a much more difficult object, which is not known in detail even for the case of vanishing background fields. For the purpose of this study and in order to make the equations tractable, we resort to a simple ansatz of the form  $\Gamma^\nu \rightarrow \gamma^\nu \Gamma(k^2)$ , where  $\Gamma(k^2)$  is taken to be independent of the magnetic field. The explicit form of  $\Gamma(k^2)$  is discussed in the Appendix. From a technical point of view, such an ansatz allows us to perform the integrations over  $x$  and  $y$  analytically, see below, and therefore makes the equations numerically feasible. More refined vertex constructions along the lines of Ref. [43] are desirable, but require a further considerable increase over the already very demanding numerical effort and therefore seem out of reach at the moment. However, from comparison with corresponding approximations at zero magnetic field, we believe

that the present truncation already allows us to deliver qualitative insights into the behavior of quarks in a magnetic background and is therefore sufficient within the scope of this work. This is discussed in more detail also in the Appendix.

The integral over  $x$ , involving a product of Ritus- and Fourier eigenfunctions, is given by

$$\int d^4x \bar{E}_p(x) \gamma^\mu E_q(x) e^{ikx}. \quad (20)$$

A similar integral for  $y$  remains to be done. If we had only particles in Ritus or in Fourier eigenfunctions at the quark-gluon vertex, this integral would be trivial due to the fact that those two systems are complete orthonormal vector spaces. We would simply obtain delta functions ensuring eigenvalue/momentum conservation. In our case however, we have interacting particles that are diagonal in different bases. Nevertheless, the integral in Eq. (20) can be done analytically. This involves the Fourier transform of a product of parabolic cylinder functions and yields

$$\begin{aligned} \int d^4x \bar{E}_p(x) \gamma^\mu E_q(x) e^{ikx} &= (2\pi)^4 \delta^{(3)}(q+k-p) e^{-k_\perp^2/4|eH|} e^{ik_1(q_2+p_2)/2eH} \\ &\times \sum_{\sigma_1, \sigma_2 = \pm} \frac{e^{i \text{sgn}(eH)(n(\sigma_1, l) - n(\sigma_2, l_q))\phi}}{\sqrt{n(\sigma_1, l)! n(\sigma_2, l_q)!}} J_{n(\sigma_1, l) n(\sigma_2, l_q)}(k_\perp) \Delta(\sigma_1) \gamma^\mu \Delta(\sigma_2) \end{aligned} \quad (21)$$

with the abbreviations

$$k_\perp^2 = k_1^2 + k_2^2, \quad n(\sigma, l) = l + \frac{\sigma}{2} \text{sgn}(eH) - \frac{1}{2}, \quad \phi = \arctan(k_2/k_1). \quad (22)$$

Furthermore,

$$J_{n_1 n_2} \equiv \sum_{m=0}^{\min(n_1, n_2)} \frac{n_1! n_2!}{m!(n_1-m)!(n_2-m)!} \left( i \text{sgn}(eH) k_\perp \frac{\sqrt{2|eH|}}{2eH} \right)^{n_1+n_2-2m}. \quad (23)$$

Composing all the bits and pieces, the quark self-energy now reads

$$\begin{aligned} \Sigma(p, p') &= (2\pi)^4 \delta^{(3)}(p-p') g^2 C_F \int \frac{d^2 q_\parallel}{(2\pi)^4} \int_{-\infty}^{\infty} dq_2 \int_{-\infty}^{\infty} dk_1 e^{-k_\perp^2/2|eH|} \sum_{\sigma_1, \sigma_2, \sigma_3, \sigma_4} \frac{e^{i \text{sgn}(eH)(n_1 - n_2 + n_3 - n_4)\phi}}{\sqrt{n_1! n_2! n_3! n_4!}} \\ &\times J_{n_1 n_2}(k_\perp) J_{n_3 n_4}(k_\perp) \Delta(\sigma_1) \gamma^\mu \Delta(\sigma_2) \frac{1}{A_\parallel(q) i\gamma \cdot q_\parallel + A_\perp(q) i\gamma \cdot q_\perp + B(q)} \\ &\times \Delta(\sigma_3) \gamma^\nu \Delta(\sigma_4) P^{\mu\nu}(k) \Gamma(k^2) D(k^2). \end{aligned} \quad (24)$$

Here, the sum over  $l_q$  counts the Landau levels and the spin projection sums over  $\sigma_{1\dots 4}$  realize their degeneracies. The expression (24) is exact with respect to the treatment of the magnetic field. Unfortunately, it is extremely difficult to

solve numerically. The reason for that lies in the form of the functions  $J_{nm}$ , as can be seen when using an alternative derivation. Starting from Eq. ((20)), it can be shown that Eq. (24) is identical to

$$\begin{aligned} \Sigma(p, p') &= (2\pi)^4 \delta^{(3)}(p - p') g^2 C_F \sum_{l_q} \int \frac{d^2 q_{\parallel}}{(2\pi)^4} \int_{-\infty}^{\infty} dq_2 \int_{-\infty}^{\infty} dk_1 e^{-k_{\perp}^2/2|eH|} \\ &\times \sum_{\sigma_1, \sigma_2, \sigma_3, \sigma_4} e^{i \text{sgn}(eH)(n_1 - n_2 + n_3 - n_4)\phi} n_1! n_3! \left( i \frac{k_{\perp}}{\sqrt{2|eH|}} \right)^{n_2 - n_1 + n_4 - n_3} L_{n_1}^{n_2 - n_1} \left( \frac{k_{\perp}^2}{2|eH|} \right) L_{n_3}^{n_4 - n_3} \left( \frac{k_{\perp}^2}{2|eH|} \right) \\ &\times \Delta(\sigma_1) \gamma^{\mu} \Delta(\sigma_2) \frac{1}{A_{\parallel}(q) i\gamma \cdot q_{\parallel} + A_{\perp}(q) i\gamma \cdot q_{\perp} + B(q)} \Delta(\sigma_3) \gamma^{\nu} \Delta(\sigma_4) P^{\mu\nu}(k) \Gamma(k^2) D(k^2), \end{aligned} \quad (25)$$

where  $L_n^m(x)$  are the generalized Laguerre polynomials. Therefore, solving Eq. (25) numerically involves an integration routine that is precise for an integrand that behaves like a polynomial of order  $n$ . According to Eq. (22),  $n$  is proportional to the number of Landau levels  $l$ , lying arbitrary close to each other for small  $eH$ , and hence a numerical treatment of the above expression is extremely hard. This is unfortunate for QCD, where in general the gluon dressing function or the quark gluon vertex are not known analytically and numerical approaches are the only available tool.

An approximation of the above expressions for small magnetic fields is discussed in [33]. Here, we follow the opposite strategy and consider the case where the magnetic field is sufficiently large [29]. To this end, note that the

integrand in the quark self-energy is given as a function of  $k_{\perp}/2|eH|$ , where large values of  $k_{\perp}$  are essentially suppressed. If the magnetic field is large, only terms up to the smallest order in  $k_{\perp}/2|eH|$  need to be kept. We adopt this approximation in the following, keeping in mind that our results will not be reliable in the small field limit.

In this approximation, the vertex is simplified drastically and given by [29]

$$J_{nm}(k_{\perp}) \rightarrow \frac{[\max(n, m)]!}{|n - m|!} (ik_{\perp}/\sqrt{2|eH|})^{|n-m|} \rightarrow n! \delta_{nm}. \quad (26)$$

One then has

$$\int d^4 x \bar{E}_p(x) \gamma^{\mu} E_q(x) e^{ikx} = (2\pi)^4 \delta^{(3)}(q + k - p) e^{-k_{\perp}^2/4|eH|} e^{ik_1(q_2 + p_2)/2eH} \sum_{\sigma_1, \sigma_2} \delta_{n(\sigma_1, l) n(\sigma_2, l_q)} \Delta(\sigma_1) \gamma^{\mu} \Delta(\sigma_2) \quad (27)$$

and thus

$$\begin{aligned} \Sigma(p, p') &= (2\pi)^4 \delta^{(3)}(p - p') i g^2 C_F \sum_{l_q=0}^{\infty} \int \frac{d^2 q_{\parallel}}{(2\pi)^4} \int_{-\infty}^{\infty} dq_2 \int_{-\infty}^{\infty} dk_1 e^{-k_{\perp}^2/2|eH|} \sum_{\sigma_1 \sigma_2 \sigma_3 \sigma_4} \delta_{n(\sigma_1, l) n(\sigma_2, l_q)} \delta_{n(\sigma_3, l_q) n(\sigma_4, l')} \\ &\times \Delta(\sigma_1) \gamma^{\mu} \Delta(\sigma_2) \frac{1}{A_{\parallel}(q) \gamma \cdot q_{\parallel} + A_{\perp}(q) \gamma \cdot q_{\perp} + B(q)} \Delta(\sigma_3) \gamma^{\nu} \Delta(\sigma_4) D(k^2) \Gamma(k^2) P^{\mu\nu}(k). \end{aligned} \quad (28)$$

As compared to the case of zero background field, which would yield a factor  $(2\pi)^4 \delta^{(4)}(q + k - p) \gamma^{\mu}$  in front of the integral, here only the momenta  $\delta^{(3)}(q + k - p) \equiv \delta(q_0 + k_0 - p_0) \delta(q_3 + k_3 - p_3) \delta(q_2 + k_2 - p_2)$  are conserved as already discussed above. In the integrand, the additional factor  $\delta_{n(\sigma_1, l) n(\sigma_2, l_q)}$  allows for transitions between adjacent Landau levels. This does not come as a surprise, since the eigensystem of the quark in an Abelian background field is supersymmetric in the sense that transitions between two neighboring Landau levels constitute spin one transitions (i.e. from  $\pm 1/2$  to  $\mp 1/2$ ). Gluons, perpendicular with respect to the magnetic field, will therefore induce such transitions, whereas longitudinal gluons do not change the Landau level of incoming and outgoing quarks at the

vertex. The  $U(1)$  field breaks the initial  $O(4)$  symmetry to an  $O(2)$  symmetry in the t-z-plane. This explains the modification of the vertex

$$\gamma^{\mu} \rightarrow \Delta(\sigma_1) \gamma^{\mu} \Delta(\sigma_2),$$

seen in Eq. (28) as compared to the zero field case.

These considerations can be easily generalized to unquenched QCD. The only difference is the appearance of an anisotropy in the gluon dressing functions, accounting for the modified behavior of the gluon polarization. We will discuss this below in Sec. IV.

The relations

$$\begin{aligned} \Delta(\sigma)\gamma_{\parallel}^{\mu} &= \gamma_{\parallel}^{\mu}\Delta(\sigma), & \Delta(\sigma)\gamma_{\perp}^{\mu} &= \gamma_{\perp}^{\mu}\Delta(-\sigma), \\ \Delta(\sigma_a)\Delta(\sigma_b) &= \Delta(\sigma_a)\delta_{ab} \end{aligned} \quad (29)$$

are useful to decompose the vertex into two contributions

$$\begin{aligned} \Delta(\sigma_1)\gamma^{\mu}\Delta(\sigma_2) &= \Delta(\sigma_1)(\gamma_{\parallel}^{\mu} + \gamma_{\perp}^{\mu})\Delta(\sigma_2) \\ &= \delta_{\sigma_1, \sigma_2}\Delta(\sigma_1)\gamma_{\parallel}^{\mu} + \delta_{\sigma_1, -\sigma_2}\Delta(\sigma_1)\gamma_{\perp}^{\mu}. \end{aligned} \quad (30)$$

Furthermore, tracing over the spin projector gives

$$\sum_{\sigma} \text{Tr}[\Delta(\sigma)] \rightarrow \chi(l) = \begin{cases} 4, & l > 0 \\ 2, & l = 0 \end{cases} \quad (31)$$

since for  $l = 0$  the fermion can only have  $\sigma = \text{sgn}(eH)$ .

After performing the traces in the quark DSE and using the abbreviation  $\int_q \equiv \int \frac{d^2 q_{\parallel}}{(2\pi)^4} \int_{-\infty}^{\infty} dq_2 dk_1$  we obtain

$$\begin{aligned} B(p)|_{l_p=l} &= Z_2 m + Z_{1f} g^2 C_F \int_q \left\{ \left( \frac{B(q)}{B^2(q) + A_{\parallel}^2(q)q_{\parallel}^2 + A_{\perp}^2(q)q_{\perp}^2} \right) \Big|_{l_q=l} e^{-k_{\perp}^2/2|eH|} \left( 2 - \frac{k_{\parallel}^2}{k^2} \right) D(k^2) \Gamma(k^2) \right\} \\ &+ \frac{g^2 C_F}{p_{\parallel}^2} \frac{2}{\chi(l)} \sum_{l_q=l\pm 1} \int_q \left\{ \left( \frac{B(q)}{B(q)^2(q) + A_{\parallel}^2(q)q_{\parallel}^2 + A_{\perp}^2(q)q_{\perp}^2} \right) \Big|_{l_q} e^{-k_{\perp}^2/2|eH|} \left( 2 - \frac{k_{\perp}^2}{k^2} \right) D(k^2) \Gamma(k^2) \right\}, \end{aligned} \quad (32)$$

where  $k_2 = q_2 - p_2$ . Although  $p_2$  appears explicitly here, it can be seen from the form of the integrand that the final result does not depend on it, as expected. Without loss of generality, we will therefore set  $p_2 = 0$ . For the vector dressing functions we find,

$$\begin{aligned} A_{\parallel}(p)|_{l_p=l} &= Z_2 - Z_{1f} \frac{g^2 C_F}{p_{\parallel}^2} \int_q \left\{ \left( \frac{A_{\parallel}(q)}{B(q)^2(q) + A_{\parallel}^2(q)q_{\parallel}^2 + A_{\perp}^2(q)q_{\perp}^2} \right) \Big|_{l_q=l} e^{-k_{\perp}^2/2|eH|} K_1(p, q) D(k^2) \Gamma(k^2) \right\} \\ &+ \frac{g^2 C_F}{p_{\parallel}^2} \frac{2}{\chi(l)} \sum_{l_q=l\pm 1} \int_q \left\{ \left( \frac{A_{\parallel}(q)}{B(q)^2(q) + A_{\parallel}^2(q)q_{\parallel}^2 + A_{\perp}^2(q)q_{\perp}^2} \right) \Big|_{l_q} e^{-k_{\perp}^2/2|eH|} K_2(p, q) D(k^2) \Gamma(k^2) \right\} \end{aligned} \quad (33)$$

with kernels

$$\begin{aligned} K_1(p, q) &= p_{\parallel} q_{\parallel} \cos(\varphi) \frac{k_{\parallel}^2}{k^2} - 2 \frac{(q_{\parallel} p_{\parallel} \cos(\varphi) - p_{\parallel}^2)(q_{\parallel}^2 - q_{\parallel} p_{\parallel} \cos(\varphi))}{k^2} \\ K_2(p, q) &= \left( 2 - \frac{k_{\perp}^2}{k^2} \right) p_{\parallel} q_{\parallel} \cos(\varphi) \end{aligned} \quad (34)$$

and  $\cos(\varphi) = \frac{\vec{p}_{\parallel} \cdot \vec{q}_{\parallel}}{|p_{\parallel}| |q_{\parallel}|}$ . Furthermore,

$$\begin{aligned} A_{\perp}(p)|_{l_p=l} &= Z_2 + Z_{1f} \frac{g^2 C_F}{p_{\parallel}^2} \int_q \left\{ \left( \frac{A_{\perp}(q)}{B(q)^2(q) + A_{\parallel}^2(q)q_{\parallel}^2 + A_{\perp}^2(q)q_{\perp}^2} \right) \Big|_{l_q=l} e^{-k_{\perp}^2/2|eH|} \left( 2 - \frac{k_{\parallel}^2}{k^2} \right) p_{\perp} q_{\perp} D(k^2) \Gamma(k^2) \right\} \\ &- \frac{g^2 C_F}{p_{\parallel}^2} \frac{2}{\chi(l)} \sum_{l_q=l\pm 1} \int_q \left\{ \left( \frac{A_{\perp}(q)}{B(q)^2(q) + A_{\parallel}^2(q)q_{\parallel}^2 + A_{\perp}^2(q)q_{\perp}^2} \right) \Big|_{l_q} e^{-k_{\perp}^2/2|eH|} \frac{k_{\perp}^2 - k_{\parallel}^2}{k^2} p_{\perp} q_{\perp} D(k^2) \Gamma(k^2) \right\}, \end{aligned} \quad (35)$$

where  $\chi(l)$  is given by Eq. (31). The renormalization factors of the quark propagator and the quark-gluon vertex are denoted by  $Z_2$  and  $Z_{1f}$ . Note that the contributions to the self-energy consist of two terms. The first one describes the radiation and emission of a ‘‘longitudinal’’ gluon which is polarized in the  $z$ - $t$ -plane, as indicated by  $= g_{\parallel}^{\mu\nu} - k_{\parallel}^{\mu} k_{\parallel}^{\nu} / k^2$ .

Such a gluon does not induce transitions between Landau levels. However, the second term corresponds to Landau level transitions, it is accompanied by a gluon  $\propto g_{\perp}^{\mu\nu} - k_{\perp}^{\mu} k_{\perp}^{\nu} / k^2$ . In the latter case the gluon emission can either increase or decrease the Landau level of the internal quark, except for the case of the lowest Landau

level, where only a transition up to the second Landau level can happen (for there are no negative Landau levels). This decomposition is a direct result of Eq. (30). Mixed terms, such as  $\Delta(\sigma_1)\gamma_{\parallel}\Delta(\sigma_2)\dots\Delta(\sigma_3)\gamma_{\perp}\Delta(\sigma_4)$ , do not appear as they would violate conservation of the Ritus eigenvalues.

Equations (33)–(35) can be solved numerically once the dressed gluon propagator and the quark-gluon vertex have been determined. As explained above, for the gluon propagator, we employ a fit to the lattice results given in Ref. [42]; for the vertex we use an ansatz that satisfies both, the correct ultraviolet running from resummed perturbation theory (with vanishing external field) and an approximate Slavnov-Taylor identity in the infrared, see Ref. [44] for details. The ansatz naturally takes into account an infrared enhancement of the quark-gluon interaction as discussed in [7]; the explicit form is given in the Appendix. Equations (33)–(35) are then solved numerically on logarithmic integration grids using standard numerical

methods. The sum over the Landau levels is carried out explicitly up to a sufficiently large number of discrete Landau levels and the remaining part of the sum is treated as an integral. Due to the dependence  $p_{\perp} \propto \sqrt{2|eH|l}$ , the density of Landau levels per energy interval grows and the error due to this approximation can be neglected, once the level spacing is sufficiently small. In practice, we use 80–100 Landau levels in the explicit summation part.

### III. RESULTS FOR QUENCHED QCD

Our results for the quark dressing functions  $A_{\perp}(p_{\perp}, p_{\parallel})$ ,  $A_{\parallel}(p_{\perp}, p_{\parallel})$  and  $B(p_{\perp}, p_{\parallel})$  are shown in Fig. 1 for magnetic fields between  $0.5 \text{ GeV}^2$  and  $4 \text{ GeV}^2$  and a renormalized current quark mass of  $m = 3.7 \text{ MeV}$  at  $\mu = 100 \text{ GeV}$ . Solid lines represent the single Landau levels, starting with  $l = 1$ . The lowest Landau levels of  $B$  and  $A_{\parallel}$  are shown in Fig. 2; the dressing function  $A_{\perp}$  is not defined on the lowest

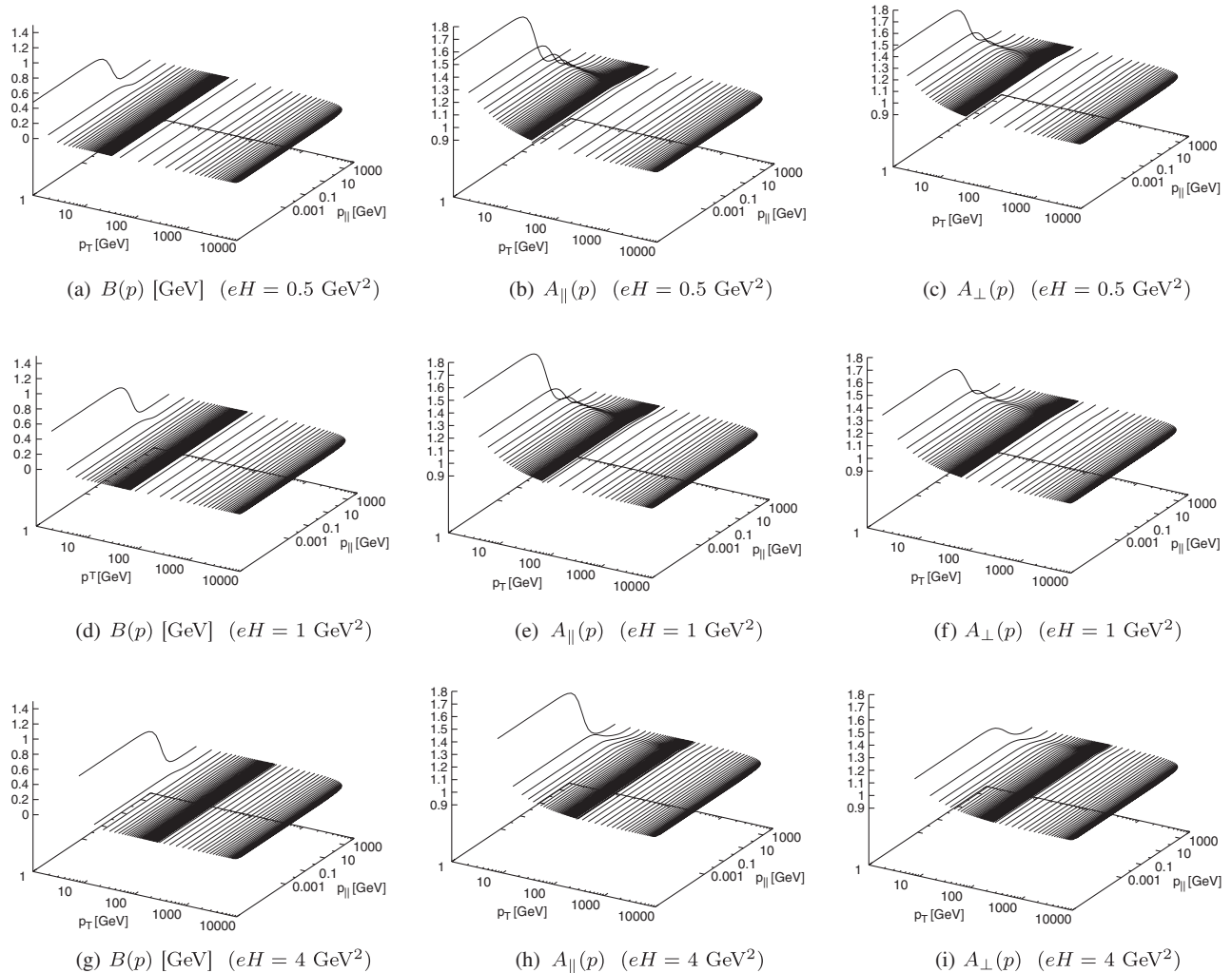


FIG. 1. Quark dressing functions for  $eH = 0.5 \text{ GeV}^2$  (first line),  $eH = 1 \text{ GeV}^2$  (second line) and  $eH = 4 \text{ GeV}^2$  (third line). Shown are the individual Landau levels as a function of  $p_{\parallel}^2$  and  $p_{\perp}^2$  starting with the second lowest level  $l = 1$ .

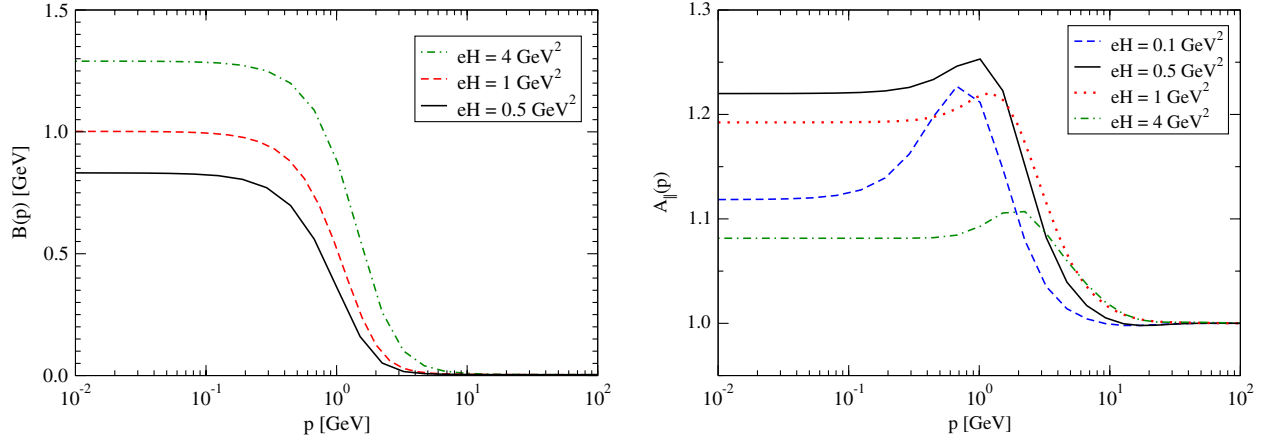


FIG. 2 (color online). Quenched dressing functions  $B$  and  $A_{\parallel}$  of the quark propagator for different magnetic fields as a function of  $p \equiv p_{\parallel}$  at a bare quark mass of  $m = 3.7$  MeV at  $\mu = 100$  GeV. Shown is the result for the lowest Landau level from a full calculation taking all Landau levels into account. The dressing function  $A_{\perp}$  is not defined on the lowest Landau level.

Landau level. Whereas the two larger values of the magnetic field are clearly in a region where we trust our approximation, the lowest value is in the region where the approximation may start to break down, see below. In general, we clearly see the influence of the magnetic field on the dressing functions. For the large fields, the lowest Landau level dominates. Note, however, that the dressing functions of the second lowest Landau level are still large and also higher Landau levels are visibly different from their bare values  $B = m$  and  $A_{\perp} = A_{\parallel} = 1$ , even at the extremely large field of  $eH = 4$  GeV<sup>2</sup> shown in the plot and beyond (we performed calculations up to  $eH = 50$  GeV<sup>2</sup>). This is true for the scalar dressing functions, but even more for the two vector components  $A_{\perp}$  and  $A_{\parallel}$ . Thus, although an approximation using the lowest Landau level may capture essential qualitative features, significant quantitative corrections remain even for large fields. We will discuss this again below.

The effects of the magnetic field on dynamical mass generation can be best seen at the lowest Landau level of the scalar dressing function in the left diagram of Fig. 2. On the one hand, we find the typical increase of the dressing function with growing magnetic field indicative for magnetic catalysis. On the other hand, the scale at which the midmomentum OPE-behavior  $B(p) \sim 1/p^2$  sets in is shifted considerably into the direction of the larger momenta. This is indicative of the additional external scale  $eH$  introduced into the system by the strong magnetic field. An interesting nonlinear dependence on  $eH$  can be seen in the infrared momentum region of  $A_{\parallel}$ . For the lowest Landau level, shown in the right diagram of Fig. 2, we find that the dressing function  $A_{\parallel}(p_{\parallel} = 0)$  first rises with growing field, then reaches a maximum and drops again for very large fields. The growth for small fields is similar to the one found in

Ref. [33], where a different approximation of the quark-DSE has been used. We find that within our truncation the value of  $A_{\parallel}(p_{\parallel} = 0)$  is maximal around  $|eH| \approx 0.5$  GeV<sup>2</sup> and then decreases monotonically with growing a field, even crossing the  $A_{\parallel}(0) = 1$  line around  $|eH| \approx 12$  GeV<sup>2</sup>. Thus, for very large fields, the dressing function even becomes smaller than the one in the infrared. We will see later in Sec. V that this is an artifact of the quenched approximation. For the higher Landau levels the nonlinear behavior of  $A_{\parallel}$  for fields around  $|eH| \approx 0.5$  GeV<sup>2</sup> is also present, but these dressing functions remain larger than one even at extremely large fields.

We now study the change of the quark condensate with the magnetic field. Using again the expansion in terms of Ritus eigenfunctions, the corresponding expression is given by

$$\begin{aligned}
 -\langle \bar{q}q \rangle &= Z_2 \lim_{x \rightarrow 0} \text{tr} S(x, 0) \\
 &= Z_2 N_c \frac{eH}{2\pi^2} \sum_{l_q=0}^{\infty} \frac{\chi(l_q)}{2} \\
 &\quad \times \int_0^{\infty} dq_{\parallel} q_{\parallel} \left( \frac{B(q)}{B^2(q) + q_{\parallel}^2 A_{\parallel}^2(q) + q_{\perp}^2 A_{\perp}^2(q)} \right) \Big|_{l_q}.
 \end{aligned} \tag{36}$$

Below, we discuss results both in the chiral limit and at a finite quark mass roughly corresponding to an up-quark. At finite bare mass, the quark condensate diverges linearly with the cutoff. This is to be contrasted with the corresponding quadratic divergence at vanishing field; the linear behavior observed here is a direct consequence of the effective dimensional reduction introduced by the magnetic field.

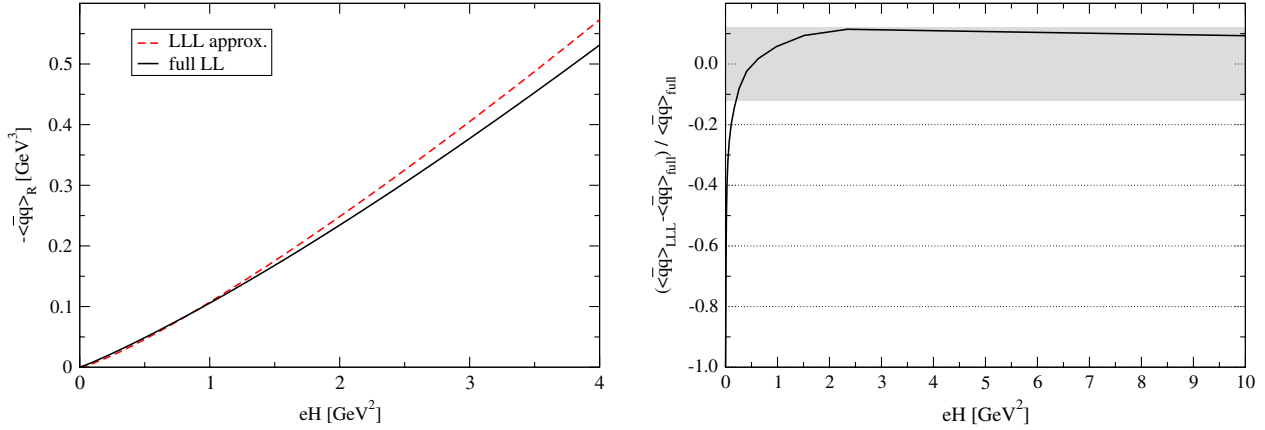


FIG. 3 (color online). Quark condensate for our full calculation compared with the lowest Landau level (LLL) approximation. On the left we display the condensate, on the right the relative difference between the condensates. The shaded region indicates a twelve percent band around zero.

$$\langle\bar{q}q\rangle_{m\neq 0} \rightarrow (\text{finite terms}) + m\Lambda. \quad (37)$$

Since the divergence is the same for all bare masses, it can be regularized by subtracting the chiral condensate of a heavy quark,

$$\langle\bar{q}q\rangle_R = \langle\bar{q}q\rangle_m - \frac{m}{m_{\text{heavy}}} \langle\bar{q}q\rangle_{\text{heavy}}. \quad (38)$$

This procedure leaves a residual term of order  $m/m_{\text{heavy}}$  in addition to the finite part of the quark condensate. This residual term can be neglected when the mass of the regulator quark gets sufficiently heavy.

The regularized quark condensate for large magnetic fields is shown in the left diagram of Fig. 3. Clearly, the condensate grows for an increasing magnetic field. This behavior is in agreement with general expectations. In particular, chiral perturbation theory ( $\chi$ PT) predicts a quadratic rise for small fields  $eH \ll m_\pi^2$ , which then turns into a linear behavior for intermediate fields  $m_\pi^2 < eH < \Lambda_{\text{QCD}}^2$  [45]. Lattice simulations in general agree with this finding, see e.g. [3,11,13,17,19]. The linear growth of the condensate with magnetic field is also observed for fields much larger than the  $\chi$ PT convergence radius  $eH > \Lambda_{\text{QCD}}^2$  [13,17,18,21,33]. For asymptotically large fields, one furthermore expects a power law  $\sim (eH)^{3/2}$  on dimensional grounds [46]. In our calculation we cannot address the region of very small fields due to the approximations made in Eq. (26). Consequently, our result for the quark condensate does not approach the zero field limit  $\langle\bar{q}q\rangle_R = 0.028 \text{ GeV}^3$  but instead goes to zero when  $eH \rightarrow 0$ . From the magnitude of the difference, one can infer that the approximation is probably good as long as  $eH \geq 0.5 \text{ GeV}^2 \approx \Lambda_{\text{QCD}}^2$ , with  $\Lambda_{\text{QCD}}$  evaluated in the minimal MOM-scheme of Ref. [47], that is also used in our calculations. This ties in with the fact that our approximation of the quark DSE follows from an expansion in  $k_\perp^2/2|eH|$ , where the largest contributions to the quark self-energy stems from momenta  $k_\perp < \Lambda_{\text{QCD}}$ . As a consequence we cannot see the

quadratic rise of the condensate for small fields predicted by chiral perturbation theory. However we do find the linear growth at intermediary fields which is supplemented by a term proportional to  $(eB)^{3/2}$  for large fields in agreement with the expectations discussed above. We come back to this discussion in Sec. V, where we present corresponding unquenched results.

In Fig. 3 we also compare our full calculation with the lowest Landau level (LLL) approximation. A particularly useful quantity is the relative difference between the two calculations shown in the right diagram of Fig. 3. As expected, for small fields the Landau levels are close to each other and the LLL approximation becomes unreliable. For fields larger than about  $eH > 0.2 \text{ GeV}^2$ , the LLL becomes reliable on the twelve percent level (indicated in grey in the diagram). This deviation persists to very large fields and decreases only very slowly: only for asymptotically large fields, the relative difference goes to zero and the LLL becomes exact.

Next, we discuss the connection of our result with the spin polarization structure of QCD. It was shown in [48], that external fields can give a handle on observables that could not be obtained otherwise. The presence of a magnetic field induces a nonzero expectation value for the tensor polarization operator  $\sigma^{\mu\nu}$  as described e.g. in Refs. [15]. In the case of a field along the z-axis,  $\langle\sigma^{12}\rangle \equiv \langle\bar{q}\sigma^{12}q\rangle$  will correspond to the average spin alignment along this quantization axis. Here, we find that  $\langle\sigma^{12}\rangle$  obtains a nonzero value even in the absence of spin dependent tensor structures in the quark propagator. In such a case, the polarization of the QCD vacuum will be caused by the special role of the lowest Landau level. The expectation value of the operator can be pictorially represented as

$$\langle\sigma^{12}\rangle = \text{Diagram}$$

The diagram shows a circular loop with an arrow indicating a clockwise direction. At the top of the loop, there is a small circle containing a cross (X), representing the tensor polarization operator  $\sigma^{12}$ .

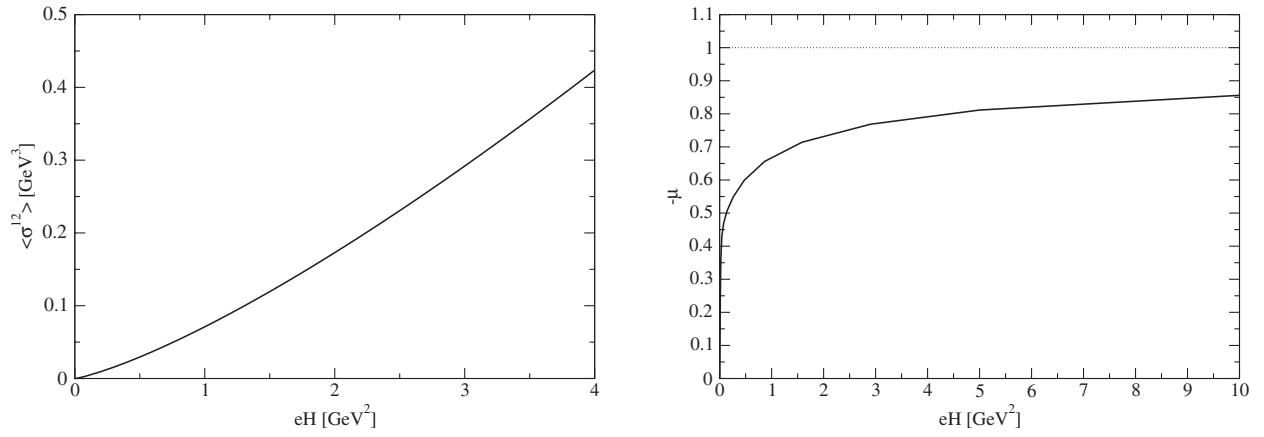


FIG. 4. Left: Regularized expectation value of the spin polarization tensor  $\langle \sigma^{12} \rangle$ . Right: Regularized magnetic polarization  $\mu$  of the QCD vacuum.

where the cross represents an insertion of  $\sigma^{12}$ . This quantity is explicitly written as

$$\begin{aligned} \langle \sigma^{12} \rangle &= Z_2 N_c \lim_{x \rightarrow 0} \int \frac{d^4 q}{(2\pi)^4} \text{Tr} \left[ \sigma^{12} E_q(x) \frac{1}{i\gamma \cdot q_{\parallel} A_{\parallel}(q) + i\gamma \cdot q_{\perp} A_{\perp}(q) + B(q)} \bar{E}_q(0) \right] \\ &= Z_2 N_c \lim_{x \rightarrow 0} \int \frac{d^4 q}{(2\pi)^4} \sum_{\substack{\sigma=\pm \\ l_q > 0}} E_{q,\sigma}(x) E_{q,\sigma}^{\dagger}(0) \text{Tr} \left[ \Delta(\sigma) \sigma^{12} \frac{B(q)}{B^2(q) + A_{\parallel}^2(q) q_{\parallel}^2 + A_{\perp}^2(q) q_{\perp}^2} \right], \end{aligned} \quad (39)$$

where  $\bar{E}_q = \gamma^0 E_q^{\dagger} \gamma^0$ . All Landau levels, except for the lowest, are degenerate with respect to the two spin directions  $\uparrow, \downarrow$ , which means that for a nonexplicit spin-dependent propagator, the contributions to  $\langle \sigma^{12} \rangle$  from higher Landau levels cancel on average, as can be seen from the form of the expectation value

$$\begin{aligned} \langle \sigma^{12} \rangle &= Z_2 N_c \frac{eH}{2\pi^2} \sum_{l_q=0}^{\infty} \int_0^{\infty} dq_{\parallel} q_{\parallel} \\ &\quad \times \sum_{\substack{\sigma=\pm \\ l_q > 0}} \left( \frac{\sigma B(q)}{B^2(q) + A_{\parallel}^2(q) q_{\parallel}^2 + A_{\perp}^2(q) q_{\perp}^2} \right) \Big|_{l_q} \\ &= Z_2 N_c \frac{eH}{2\pi^2} \int_0^{\infty} dq_{\parallel} q_{\parallel} \frac{\Delta \text{sgn}(eH) B(q)}{B^2(q) + A_{\parallel}^2(q) q_{\parallel}^2}. \end{aligned} \quad (40)$$

This quantity behaves in analogy to the chiral condensate in terms of regularization, simply because the inserted operator  $\sigma^{12}$  is dimensionless. Therefore the regularized quantity can be defined as

$$\langle \sigma^{12} \rangle_R = \langle \sigma^{12} \rangle_m - \frac{m}{m_{\text{heavy}}} \langle \sigma^{12} \rangle_{\text{heavy}}, \quad (41)$$

where  $m_{\text{heavy}}$  is a heavy mass as before.

Our results for  $\langle \sigma^{12} \rangle$  as a function of the external field is shown in the left diagram of Fig. 4. Similar to the quark condensate, the magnetic moment  $\langle \sigma^{12} \rangle$  follows a power law with a linear term and a term  $\sim (eH)^{3/2}$ . The polarization  $\mu$  of the QCD vacuum

$$\mu = \frac{\langle \sigma^{12} \rangle}{\langle \bar{q}q \rangle}, \quad (42)$$

tends to one in the large field limit, indicating the similarity of the coefficient in front of the term  $\sim (eH)^{3/2}$ . Since  $\langle \sigma^{12} \rangle$  extracts the contribution of the lowest Landau level to the chiral condensate, this limit is driven by the lowest Landau level. In line with the results discussed above we find that this saturation only sets in at very large, if not asymptotic fields.

For completeness, note that the spin tensor expectation value can be expanded into operators

$$\langle \sigma^{12} \rangle = \chi \langle \bar{q}q \rangle eH + O(eH^2), \quad (43)$$

where terms  $\propto O(eH^0)$  need to vanish, since the QCD vacuum in the zero field case is isotropic and therefore unpolarized. For small fields  $eH$ , the magnetic susceptibility  $\chi$  is given by

$$\chi \approx \frac{\langle \sigma^{12} \rangle}{\langle \bar{q}q \rangle} \frac{1}{eH} = \frac{\mu}{eH}. \quad (44)$$

Since our approximation tends to break down in the small field limit, the magnetic susceptibility is not well accessible in our scheme and we will refrain from attempting to give an extrapolated result.

#### IV. UNQUENCHED DSES': FORMALISM

In this section, we establish the techniques necessary to formulate unquenched QCD in a magnetic field combining the Ritus method with the Dyson Schwinger approach.

Although gluons do not couple directly to the external Abelian field, they are affected by its presence via the quark loop in the gluon DSE. Due to their coupling to charged quarks, the gluons inherit the anisotropy introduced by the magnetic field. Indeed, a magnetic field will modify  $\Pi^{\mu\nu}$  in a nontrivial way. We will use an orthogonal basis for the gluon polarization tensor [49–51] that is well suited to accommodate for this effect.

### A. Gluon polarization tensor

There are four linear independent vectors which can be constructed from  $k^\mu$ ,  $F^{\mu\nu}$  and the dual field strength tensor  $*F^{\mu\nu}$

$$k^\mu, \quad F^{\mu\nu}k_\nu, \quad F^{\mu\nu}F_{\nu\alpha}k^\alpha, \quad *F^{\mu\nu}k_\nu. \quad (45)$$

Similarly one can find four independent (pseudo)scalar structures

$$\frac{1}{4}F^{\mu\nu}F_{\mu\nu}, \quad \frac{1}{4}*F^{\mu\nu}, \quad k^2, \quad (k_\nu F^{\nu\mu})^2, \quad (46)$$

which all contain an even number of the antisymmetric tensors  $F^{\mu\nu}$  and  $*F^{\mu\nu}$ . The symmetric polarization tensor  $\Pi^{\mu\nu}$  contains by construction ten independent components. Furthermore, Furry's theorem [52] tells us that all components of  $\Pi^{\mu\nu}$  with an odd number of  $F_{\mu\nu}$  vanish. The dressings of these components depend only on the even structures Eq. (46) and are therefore also even. Thus, it follows that only even combinations of the vectors Eq. (45) are allowed, which reduces the number of possible tensors to six. Finally, these have to satisfy the Ward-identity  $\Pi^{\mu\nu}k_\nu = 0$  and we are left with four possible linear independent basis tensors [51].

Finding those is essentially an eigenvalue problem.  $\Pi^{\mu\nu}$  has four orthogonal eigenvectors  $b_i^\mu$  with corresponding eigenvalues

$$\kappa_i = \kappa_i \left( \frac{1}{4}F^{\mu\nu}F_{\mu\nu}, \frac{1}{4}*F^{\mu\nu}, k^2, (k_\nu F^{\nu\mu})^2 \right). \quad (47)$$

Having solved the eigenvalue problem, the polarization tensor can be written in its eigenbasis

$$\Pi^{\mu\nu}(k, k') = (2\pi)^4 \delta^{(4)}(k' - k) \Pi^{\mu\nu}(k), \quad (48)$$

$$\Pi^{\mu\nu}(k) = \sum_{i=0}^3 \kappa_i \frac{b_i^\mu b_i^\nu}{(b_i)^2}. \quad (49)$$

The first eigenvector is  $b_0^\mu = k^\mu$  with eigenvalue 0, since  $\Pi^{\mu\nu}k_\nu = 0$ . The other eigenvectors are (see [49])

$$b_1^\mu = (F^{\mu\nu}F_{\nu\rho}k^\rho)k^2 - k^\mu(k_\nu F^{\nu\alpha}F_{\alpha\beta}k^\beta), \quad (50)$$

$$b_2^\mu = *F^{\mu\nu}k_\nu, \quad (51)$$

$$b_3^\mu = F^{\mu\nu}k_\nu, \quad (52)$$

from which it is found that the projectors along those eigenvectors look like

$$\begin{aligned} \frac{b_2^\mu b_2^\nu}{(b_2)^2} &= \frac{\tilde{k}_\parallel^\mu \tilde{k}_\parallel^\nu}{\tilde{k}_\parallel^2} = \left( \delta_\parallel^{\mu\nu} - \frac{k_\parallel^\mu k_\parallel^\nu}{k_\parallel^2} \right) \equiv P_\parallel^{\mu\nu}, \\ \frac{b_3^\mu b_3^\nu}{(b_3)^2} &= \frac{\tilde{k}_\perp^\mu \tilde{k}_\perp^\nu}{\tilde{k}_\perp^2} = \left( \delta_\perp^{\mu\nu} - \frac{k_\perp^\mu k_\perp^\nu}{k_\perp^2} \right) \equiv P_\perp^{\mu\nu}, \end{aligned} \quad (53)$$

where we have defined the orthogonal momenta (being orthogonal to its corresponding partner, e.g.  $\tilde{k}_\parallel \perp k_\parallel$  and similar for  $\tilde{k}_\perp$ )

$$\tilde{k}_\parallel^\alpha = \epsilon_\parallel^{\alpha\beta} k_\parallel^\beta \quad \alpha, \beta = 0, 3, \quad (54)$$

$$\tilde{k}_\perp^\alpha = \epsilon_\perp^{\alpha\beta} k_\perp^\beta \quad \alpha, \beta = 1, 2, \quad (55)$$

with  $\epsilon_\perp^{12} = -\epsilon_\perp^{21} = 1$ ,  $\epsilon_\perp^{11} = \epsilon_\perp^{22} = 0$  and correspondingly  $\epsilon_\parallel^{30} = -\epsilon_\parallel^{03} = 1$ ,  $\epsilon_\parallel^{33} = \epsilon_\parallel^{00} = 0$ . Obviously,  $k_i^\mu \tilde{k}_j^\mu = 0$  ( $i, j = \perp, \parallel$ ) and further  $k_i^2 = \tilde{k}_i^2$ . For a constant magnetic field, the last tensor structure is easily found

$$\frac{b_1^\mu b_1^\nu}{(b_1)^2} = \frac{(k_\perp^2 k_\parallel^\mu - k_\parallel^2 k_\perp^\mu)(k_\perp^2 k_\parallel^\nu - k_\parallel^2 k_\perp^\nu)}{k_\parallel^2 k_\perp^2 k^2} \equiv P_0^{\mu\nu}. \quad (56)$$

Note that because of the completeness of the basis, we can write

$$\delta^{\mu\nu} = P_0^{\mu\nu} + P_\parallel^{\mu\nu} + P_\perp^{\mu\nu} + P_L^{\mu\nu}, \quad (57)$$

where  $P_L^{\mu\nu} = k^\mu k^\nu / k^2$ . The structures  $P_\parallel^{\mu\nu}$ ,  $P_\perp^{\mu\nu}$  and  $P_0^{\mu\nu}$  constitute a complete orthonormal basis for the transverse subspace  $P^{\mu\nu}$ . The transverse subspace is defined by

$$P^{\mu\nu} = \delta^{\mu\nu} - \frac{k^\mu k^\nu}{k^2} = P_0^{\mu\nu} + P_\parallel^{\mu\nu} + P_\perp^{\mu\nu}, \quad (58)$$

and therefore,  $P_0^{\mu\nu}$  has an alternative expression to Eq. (56)

$$P_0^{\mu\nu} = \delta^{\mu\nu} - \frac{k^\mu k^\nu}{k^2} - \frac{\tilde{k}_\parallel^\mu \tilde{k}_\parallel^\nu}{\tilde{k}_\parallel^2} - \frac{\tilde{k}_\perp^\mu \tilde{k}_\perp^\nu}{\tilde{k}_\perp^2} = \frac{k_\parallel^\mu k_\parallel^\nu}{k_\parallel^2} + \frac{k_\perp^\mu k_\perp^\nu}{k_\perp^2} - \frac{k^\mu k^\nu}{k^2}, \quad (59)$$

which is easier to use in certain calculations. The basis properties of the projectors found here can be seen from

$$P_i^{\mu\alpha} P_j^{\alpha\nu} = \delta_{ij} P^{\mu\nu}, \quad P_i^{\mu\mu} = 1. \quad (60)$$

With Eqs. (53)–(60), the most general form of the gluon propagator in the presence of an external magnetic field along the z-axis is given by

$$\begin{aligned} D^{\mu\nu}(k, k') &= (2\pi)^4 \delta^{(4)}(k' - k) \\ &\times \left( \frac{Z_0}{k^2} P_0^{\mu\nu}(k) + \frac{Z_\parallel}{k^2} P_\parallel^{\mu\nu}(k) + \frac{Z_\perp}{k^2} P_\perp^{\mu\nu}(k) \right). \end{aligned} \quad (61)$$

The inverse propagator follows as

$$D^{-1\mu\nu}(k, k') = (2\pi)^4 \delta^{(4)}(k' - k) k^2 (Z_0^{-1} P_0^{\mu\nu}(k) + Z_{\parallel}^{-1} P_{\parallel}^{\mu\nu}(k) + Z_{\perp}^{-1} P_{\perp}^{\mu\nu}(k)), \quad (62)$$

with the gluon dressing functions  $Z_i$ . In terms of the eigenvalues  $\kappa_i$  from Eq. (47), these are formally given by

$$Z_i \equiv \frac{1}{1 - \kappa_i/k^2} \quad i \in \{0, \parallel, \perp\}. \quad (63)$$

This form of the gluon propagator illustrates an important effect, which was introduced as ‘‘vacuum birefringence’’ in [53], denoting the nondegeneracy of the physical gluon modes. Stated otherwise, the refractive indices of different gluon polarizations deviate from each other.

### B. The gluon Dyson—Schwinger equation

In order to solve the DSE for the gluon propagator in an external magnetic field, we resort to an approximation introduced in Ref. [44] in the context of finite temperature and chemical potential. There, the right-hand side of the gluon DSE has been split into a part containing the gluon self-interaction and the coupling to a ghost antighost pair (‘‘Yang—Mills part’’) and the quark-loop. The Yang—Mills part, together with the bare term, has been approximated by quenched lattice results for the propagator, whereas the quark loop has been treated dynamically together with the quark DSE. We have assessed the quality of this approximation for the case of zero magnetic field using the truncation of Ref. [54]. There, the fully back-coupled system of DSEs for the gluon and quark propagators has been solved for the quenched case as well as  $N_f = 3$  quark flavors using several truncations for the quark-gluon vertex. We repeated these calculations for the vertex model used in this work and compared the results with an approximation, where the Yang—Mills part together with the bare term has been replaced by the quenched gluon propagator. We have found mild deviations between the two results only in the mid-momentum regime, where they amount to an error of less than five percent [55]. For the exploratory calculation presented in this work, this is certainly acceptable.

The resulting Dyson—Schwinger equation for the gluon propagator is displayed in Fig. 5 and given by

$$D_{\mu\nu}^{-1}(k) = D_{(0)\mu\nu}^{-1}(k) + \Pi_{\mu\nu}^g(k) + \Pi_{\mu\nu}^q(k) \approx D_{\mu\nu}^{-1\text{eff}}(k) + \Pi_{\mu\nu}^q(k). \quad (64)$$

$$\begin{aligned} \Pi^{\mu\nu}(k, k') &= -(2\pi)^4 \delta^{(3)}(k - k') \frac{g^2}{2} \sum_{l, l'} \int \frac{d^2 q_{\parallel}}{(2\pi)^4} \int_{-\infty}^{\infty} dq_2 e^{-\frac{k_{\perp}^2 + k'^2}{4eH}} e^{i(k_1' - k_1)q_2/eH} e^{-i(k_1' - k_1)k_2'/2eH} \\ &\quad \times \sum_{\sigma_1, \sigma_2, \sigma_3, \sigma_4} \delta_{n_1(l', \sigma_1) n_2(l, \sigma_2)} \delta_{n_3(l', \sigma_3) n_4(l, \sigma_4)} \text{tr}[\Delta_1 \gamma^{\mu} \Delta_2 S(q) \Delta_3 \gamma^{\nu} \Delta_4 S(q')] \Gamma(\hat{q}_{\parallel}). \end{aligned} \quad (68)$$

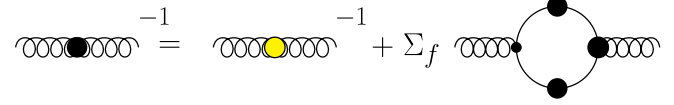


FIG. 5 (color online). Pictographic representation of the approximation of Ref. [44] for the unquenched gluon propagator.

Here, the quenched contributions are denoted by  $D_{\mu\nu}^{-1\text{eff}}(k)$  and the yellow dot in Fig. 5. Within this approximation, the effective propagator in Eq. (64) is taken to be isotropic with respect to its polarization which is well justified when realizing that there is no direct appearance of charged particles in this sector.

In order to include the effect of the magnetic field onto the gluon sector, the Ritus method will be employed for the quark loop in the gauge boson self-energy. The quark part of the gluon polarization reads

$$\Pi_{\mu\nu}^q(x, y) = -\frac{g^2}{2} \text{tr}[\gamma_{\mu} S(x, y) \Gamma_{\nu}(y) S(y, x)]. \quad (65)$$

Any part of the gluon self-energy is diagonal in Fourier space

$$\begin{aligned} \Pi_{\mu\nu}^q(k, k') &= \int d^4 x d^4 y e^{-i(kx - k'y)} \Pi_{\mu\nu}^q(x, y) \\ &= (2\pi)^4 \delta^{(4)}(k - k') \Pi^{\mu\nu}(k), \end{aligned} \quad (66)$$

and explicitly given in terms of the Ritus representation for the quark propagator  $S(x, y)$  [cf. Eq. (18)],

$$\begin{aligned} \Pi^{\mu\nu}(k, k') &= -\frac{g^2}{2} \int \frac{d^4 q}{(2\pi)^4} \int \frac{d^4 q'}{(2\pi)^4} \text{tr} \\ &\quad \times \left( \left[ \int d^4 x \bar{E}_{q'}(x) \gamma^{\mu} E_q(x) e^{-ikx} \right] \right. \\ &\quad \left. \times S(q) \left[ \int d^4 y \bar{E}_q(y) \Gamma^{\nu}(y) E_{q'}(y) e^{ik'y} \right] S(q') \right). \end{aligned} \quad (67)$$

Here,  $S(q)$  denotes the quark propagator in Ritus space. Again, the simplifications leading to Eq. (27) are employed, rendering also the gluon polarization tensor potentially unreliable at small magnetic fields,

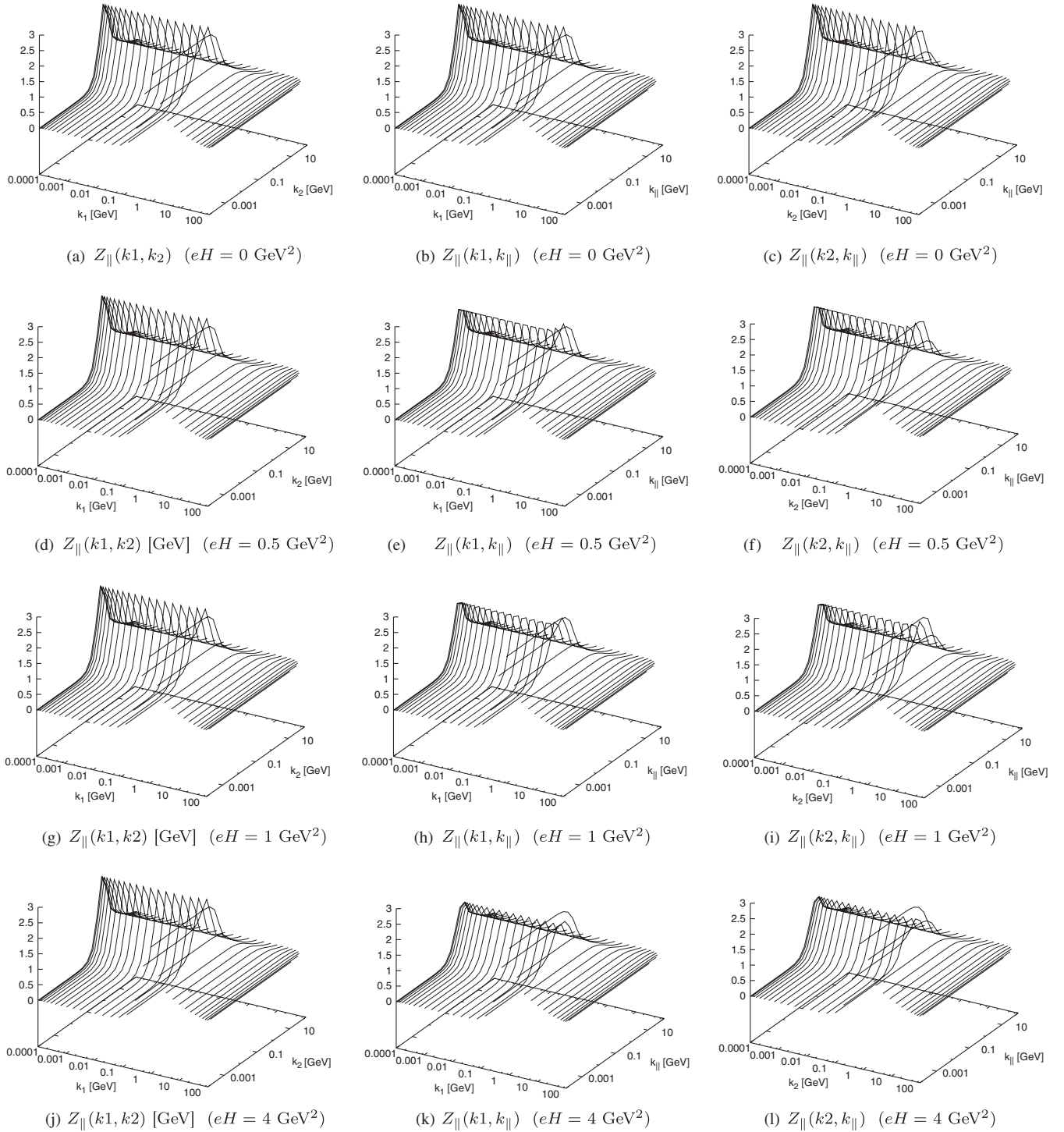


FIG. 6. Gluon dressing function  $Z_{||}(k_1, k_2, k_{||})$  for  $eH = 0 \text{ GeV}^2$  (quenched, first line),  $eH = 0.5 \text{ GeV}^2$  (second line),  $eH = 1 \text{ GeV}^2$  (third line) and  $eH = 4 \text{ GeV}^2$  (fourth line) and different momentum slices, where the third momentum is set to zero, respectively.

with  $\hat{q}_{||} = q_{||}^2 + (q'_{||})^2 + k_{\perp}^2$  and  $\Delta_i = \Delta(\sigma_i)$ . For the quark-gluon vertex, we used the same truncation as in the quenched case,  $\Gamma_{\nu}(q, q') = \gamma_{\nu}\Gamma(\hat{q}_{||})$ . However, the argument of the model dressing function  $\Gamma$  was adapted such

that the vertex is symmetric under the exchange of the two quarks and the equation remains multiplicative renormalizable, see Ref. [54] for details. The expression Eq. (68) is apparently diagonal in  $k_{||}$  and  $k_2$ . By using

$$\int_{-\infty}^{\infty} dq_2 e^{i(k_1' - k_1)q_2/eH} = 2\pi\delta(k_1' - k_1)eH, \quad (69)$$

the anticipated diagonality can be made more obvious and we obtain

$$\Pi^{\mu\nu}(k, k') = (2\pi)^4 \delta^{(4)}(k' - k) \Pi^{\mu\nu}(k) \quad (70)$$

$$\begin{aligned} \Pi^{\mu\nu}(k) = & 2\pi \frac{g^2}{2} eH \sum_{l, l'} \int \frac{d^2 q_{\parallel}}{(2\pi)^4} \left\{ e^{-k_{\perp}^2/2|eH|l} \Gamma(\hat{q}_{\parallel}^2) \right. \\ & \left. \times \sum_{\{\sigma_i\}} \delta_{n_1 n_2} \delta_{n_3 n_4} \text{tr}[\Delta_1 \gamma^{\mu} \Delta_2 S(q) \Delta_3 \gamma^{\nu} \Delta_4 S(q')] \right\}. \end{aligned} \quad (71)$$

The relationship between  $q$  and  $q'$  is given by

$$\begin{aligned} q'_0 &= q_0 - k_0, & q'_3 &= q_3 - k_3, \\ q'_{\perp} &= \sqrt{2|eH|l'}, & q_{\perp} &= \sqrt{2|eH|l}. \end{aligned} \quad (72)$$

We define

$$\begin{aligned} \mathcal{D}(q, q') = & [B^2(q) + A_{\parallel}^2(q)q_{\parallel}^2 + A_{\perp}^2(q)q_{\perp}^2][B^2(q') \\ & + A_{\parallel}^2(q')q'_{\parallel}{}^2 + A_{\perp}^2(q')q'_{\perp}{}^2]. \end{aligned} \quad (73)$$

The trace in Eq. (71) can be performed easily, yielding

$$\text{tr}[\Delta_1 \gamma^{\mu} \Delta_2 S(q) \Delta_3 \gamma^{\nu} \Delta_4 S(q')] = \frac{T_1^{\mu\nu} + T_2^{\mu\nu} + T_3^{\mu\nu}}{\mathcal{D}(q, q')}, \quad (74)$$

where

$$\begin{aligned} T_1^{\mu\nu} &= 2B(q)B(q') \\ &\times (\delta_{\parallel}^{\mu\nu} \delta_{\sigma_1, \sigma_2} \delta_{\sigma_3, \sigma_4} \delta_{\sigma_1, \sigma_3} + \delta_{\perp}^{\mu\nu} \delta_{\sigma_1, -\sigma_2} \delta_{\sigma_3, -\sigma_4} \delta_{\sigma_1, -\sigma_3}) \\ T_2^{\mu\nu} &= 2A_{\perp}(q)A_{\perp}(q')(q_{\perp} q'_{\perp} \delta_{\parallel}^{\mu\nu} \delta_{\sigma_1, \sigma_2} \delta_{\sigma_3, \sigma_4} \delta_{\sigma_1, -\sigma_3} \\ &+ [q_{\perp} q'_{\perp} \delta_{\perp}^{\mu\nu} - 2q_{\perp}^{\mu} q'_{\perp}{}^{\nu}] \delta_{\sigma_1, -\sigma_2} \delta_{\sigma_3, -\sigma_4} \delta_{\sigma_1, \sigma_3}) \\ T_3^{\mu\nu} &= 2A_{\parallel}(q)A_{\parallel}(q')([q_{\parallel} \cdot q'_{\parallel} \delta_{\parallel}^{\mu\nu} - 2q_{\parallel}^{\nu} q'_{\parallel}{}^{\mu}] \delta_{\sigma_1, \sigma_2} \delta_{\sigma_3, \sigma_4} \delta_{\sigma_1, \sigma_3} \\ &+ q_{\parallel} \cdot q'_{\parallel} \delta_{\perp}^{\mu\nu} \delta_{\sigma_1, -\sigma_2} \delta_{\sigma_3, -\sigma_4} \delta_{\sigma_1, -\sigma_3}). \end{aligned} \quad (75)$$

Inserting these three expressions in Eq. (71), we find similar properties as for the quark self-energy above: when combining the Kronecker deltas, the Landau level transitions appear

$$\begin{aligned} & \delta_{n_1(l', \sigma_1) n_2(l, \sigma_2)} \delta_{n_3(l', \sigma_3) n_4(l, \sigma_4)} \delta_{\sigma_1, \sigma_2} \delta_{\sigma_3, \sigma_4} \delta_{\sigma_1, \pm \sigma_3} \\ & \propto \delta_{l, l'} \delta_{n_1(l', \sigma_1) n_2(l, \sigma_2)} \delta_{n_3(l', \sigma_3) n_4(l, \sigma_4)} \delta_{\sigma_1, -\sigma_2} \delta_{\sigma_3, -\sigma_4} \delta_{\sigma_1, \mp \sigma_3} \\ & \propto \delta_{|l+\sigma_1 \text{sgn}(eH), l'}. \end{aligned} \quad (76)$$

Thus, either the gluon splits into a quark-antiquark pair on the same Landau level, or it induces a transition from

one Landau level to the next. Other cases are not compatible with the spin-one-boson nature of the gluon.

Putting everything together, the gluon DSE reads

$$\begin{aligned} & k^2(Z_0^{-1}(k)P_0^{\mu\nu} + Z_{\parallel}^{-1}(k)P_{\parallel}^{\mu\nu} + Z_{\perp}^{-1}(k)P_{\perp}^{\mu\nu}) \\ & = k^2 Z^{-1}(k)P^{\mu\nu} - \pi g^2 eH e^{-k_{\perp}^2/2|eH|} \\ & \times \sum_{l, l'} \int \frac{d^2 q_{\parallel}}{(2\pi)^4} \Gamma(\hat{q}_{\parallel}^2) \sum_{\{\sigma_i\}} \delta_{n_1 n_2} \delta_{n_3 n_4} \frac{T_1^{\mu\nu} + T_2^{\mu\nu} + T_3^{\mu\nu}}{\mathcal{D}(q, q')}. \end{aligned} \quad (77)$$

The equation can be decomposed into its contributions from the polarization subspaces denoted by  $P_{\perp}^{\mu\nu}$ ,  $P_{\parallel}^{\mu\nu}$  and  $P_0^{\mu\nu}$ . In the following,  $Z(k)$  stands for the dressing function of the quenched isotropic gluon propagator. The resulting equations for the dressing functions for the full gluon propagator read in a compact notation (here we have one quark flavor,  $N_f = 1$ , with charge  $q_f = e$  for brevity, although later on we solve for  $N_f = 1 + 1$  up- and down-quarks with charges  $q_f = +2/3e$  and  $q_f = -1/3e$ , respectively).

$$Z_{\parallel}^{-1}(k) = Z^{-1}(k) - \beta \sum_l \int \frac{d^2 q_{\parallel}}{(2\pi)^4} \frac{\chi(l)}{2} \frac{M_{\parallel}(q, q')}{\mathcal{D}(q, q')} \Big|_{l'=l} \Gamma(\hat{q}_{\parallel}^2), \quad (78)$$

$$\begin{aligned} Z_{\perp}^{-1}(k) = & Z^{-1}(k) - \beta \sum_l \int \frac{d^2 q_{\parallel}}{(2\pi)^4} \sum_{l'=\pm 1, l' \geq 0} \frac{N_{\perp}(q, q')}{\mathcal{D}(q, q')} \\ & \times \Gamma(\hat{q}_{\parallel}^2), \end{aligned} \quad (79)$$

$$\begin{aligned} Z_0^{-1}(k) = & Z^{-1}(k) - \beta \sum_l \int \frac{d^2 q_{\parallel}}{(2\pi)^4} \left\{ \frac{\chi(l)}{2} \frac{M_0(q, q')}{\mathcal{D}(q, q')} \Big|_{l'=l} \right. \\ & \left. + \sum_{l'=\pm 1, l' \geq 0} \frac{N_0(q, q')}{\mathcal{D}(q, q')} \right\} \Gamma(\hat{q}_{\parallel}^2). \end{aligned} \quad (80)$$

Here,  $\beta = \beta(k, eH) \equiv 2\pi g^2 q_f H e^{-k_{\perp}^2/2|eH|}$ ,  $q'_{\parallel} = q_{\parallel} - k_{\parallel}$  and  $\mathcal{D}(q, q')$  as in Eq. (73). The factor  $\frac{\chi(l)}{2}$  again accounts for the spin degeneracy of the Landau levels, which is equal to one for the lowest level but equal to two otherwise. We have defined

$$\begin{aligned} M_{\parallel}(q, q') = & A_{\perp}(q)A_{\perp}(q')q_{\perp} q'_{\perp} \\ & + A_{\parallel}(q)A_{\parallel}(q')(q_{\parallel} \cdot q'_{\parallel} - 2q_{\parallel}^2 \sin^2(\phi)), \end{aligned} \quad (81)$$

$$\begin{aligned} N_{\perp}(q, q') = & A_{\perp}(q)A_{\perp}(q')q_{\perp} q'_{\perp} \left( 1 - 2 \frac{k_{\perp}^2}{k_{\perp}^2} \right) \\ & + A_{\parallel}(q)A_{\parallel}(q')q_{\parallel} \cdot q'_{\parallel}, \end{aligned} \quad (82)$$

$$\begin{aligned} M_0(q, q') = & A_{\perp}(q)A_{\perp}(q')q_{\perp} q'_{\perp} \frac{k_{\perp}^2}{k^2} + A_{\parallel}(q)A_{\parallel}(q') \\ & \times \left( q_{\parallel} \cdot q'_{\parallel} \frac{k_{\perp}^2}{k^2} - 2 \frac{q_{\parallel} \cdot k_{\parallel} q'_{\parallel} \cdot k_{\parallel}}{k^2} \frac{k_{\perp}^2}{k_{\parallel}^2} \right), \end{aligned} \quad (83)$$

$$\begin{aligned}
 N_0(q, q') &= A_\perp(q)A_\perp(q')q_\perp q'_\perp \left( \frac{k_\parallel^2}{k^2} - 2 \frac{k_\perp^2 k_\parallel^2}{k^2 k_\perp^2} \right) \\
 &\quad + A_\parallel(q)A_\parallel(q')q_\parallel \cdot q'_\parallel \frac{k_\parallel^2}{k^2}. \quad (84)
 \end{aligned}$$

Naively, also terms proportional to  $B(q)B(q')$  may appear. However, it is clear from the  $H = 0$  case that these terms disappear after renormalization [54], such that we dropped them in the first place. Note that  $Z_\parallel(k)$  only gets contributions from similar Landau levels  $l' = l$ , whereas  $Z_\perp(k)$  only gets contributions from the neighboring ones, where  $l' = l \pm 1$ . The third dressing function  $Z_0$  receives contributions from both cases.

The gluon polarization tensor decomposition affects the structure of the quark self-energy, too. With the abbreviations

$$\int_q \equiv \int \frac{d^2 q_\parallel}{(2\pi)^4} \int_{-\infty}^{\infty} dq_2 dk_1 \quad \text{and} \quad D_q(q) \equiv B^2(q) + A_\parallel^2(q)q_\parallel^2 + A_\perp^2(q)q_\perp^2,$$

the quark DSE then reads

$$\begin{aligned}
 B(p) &= m + g^2 C_F \int_q \frac{B(q)}{D_q(q)} e^{-k_\perp^2/2|eH|} \Gamma(k^2) \\
 &\quad \times \left( \frac{Z_\parallel(k)}{k^2} + \frac{k_\perp^2 Z_0(k)}{k^2} \right) \\
 &\quad + \frac{2}{\chi(l)} g^2 C_F \sum_{l_q=l\pm 1, l_q \geq 0} \int_q \frac{B(q)}{D_q(q)} e^{-k_\perp^2/2|eH|} \Gamma(k^2) \\
 &\quad \times \left( \frac{Z_\perp(k)}{k^2} + \frac{k_\parallel^2 Z_0(k)}{k^2} \right), \quad (85)
 \end{aligned}$$

$$\begin{aligned}
 A_\parallel(p) &= 1 - g^2 C_F \int_q \frac{A_\parallel(q)}{D_q(q)} \frac{e^{-k_\perp^2/2|eH|}}{p_\parallel^2} \Gamma(k^2) \\
 &\quad \times \left( \frac{Z_\parallel(k)}{k^2} K_1(p, q) + \frac{Z_0(k)}{k^2} K_2(p, q) \right) \\
 &\quad + \frac{2}{\chi(l)} g^2 C_F \sum_{l_q=l\pm 1, l_q \geq 0} \int_q \frac{A_\parallel(q)}{D_q(q)} \frac{e^{-k_\perp^2/2|eH|}}{p_\parallel^2} \Gamma(k^2) \\
 &\quad \times \left( \frac{Z_\perp(k)}{k^2} p_\parallel \cdot q_\parallel + \frac{Z_0(k)}{k^2} p_\parallel \cdot q_\parallel \frac{k_\parallel^2}{k^2} \right), \quad (86)
 \end{aligned}$$

with kernels

$$K_1(p, q) = 2 \frac{(p_\parallel q_\parallel \sin(\phi))^2}{k_\parallel^2} - p_\parallel \cdot q_\parallel \quad (87)$$

$$K_2(p, q) = 2 \frac{k_\perp^2 p_\parallel \cdot k_\parallel q_\parallel \cdot k_\parallel}{k_\parallel^2 k^2} - p_\parallel \cdot q_\parallel \frac{k_\perp^2}{k^2}. \quad (88)$$

Furthermore,

$$\begin{aligned}
 A_\perp(p) &= 1 + g^2 C_F \int_q \frac{A_\perp(q)}{D_q(q)} \frac{e^{-k_\perp^2/2|eH|}}{p_\perp^2} \Gamma(k^2) \\
 &\quad \times \left( \frac{Z_\parallel(k)}{k^2} p_\perp q_\perp + \frac{Z_0(k)}{k^2} p_\perp q_\perp \frac{k_\perp^2}{k^2} \right) \\
 &\quad + \frac{2}{\chi(l)} g^2 C_F \sum_{l_q=l\pm 1, l_q \geq 0} \int_q \frac{A_\perp(q)}{D_q(q)} \frac{e^{-k_\perp^2/2|eH|}}{p_\perp^2} \Gamma(k^2) \\
 &\quad \times \left( \frac{Z_\perp(k)}{k^2} p_\perp q_\perp \left( 1 - 2 \frac{k_\perp^2}{k_\perp^2} \right) + \frac{Z_0(k)}{k^2} p_\perp q_\perp \right) \\
 &\quad \times \left( \frac{k_\parallel^2}{k^2} - 2 \frac{k_\parallel^2 k_\perp^2}{k_\perp^2 k^2} \right). \quad (89)
 \end{aligned}$$

Equations (78)–(80) and (85)–(90) are coupled and need to be solved simultaneously. The dressing functions  $A_\parallel$ ,  $A_\perp$  and  $B$  are functions of the scalar variables  $p_\parallel^2$  and  $p_\perp^2$ , whereas the gluon dressing functions depend on  $k_\parallel^2$ ,  $k_\perp^2$  and  $k^2$ .

For the large fields studied here, the lowest Landau level approximation is trustworthy on the ten percent level, cf. the discussion in Sec. III. In order to limit the huge numerical effort necessary to solve the coupled gluon and quark DSE self-consistently we restrict ourselves to the following scheme: we back-couple only the lowest Landau level of the quark onto the lowest Landau level of the gluon propagator and treat all other Landau levels of the gluon in quenched approximation. In this way we consistently unquench only the lowest Landau level of the gluon propagator. For the dressing functions in Eqs. (78)–(80) this means that  $Z_\perp$  stays quenched completely (since it receives only contributions from neighboring Landau levels), whereas in  $Z_\parallel$  the lowest Landau level becomes modified. The same contribution for  $Z_0$  needs a separate discussion: In order to solve three equations for the gluon dressing functions numerically, they need to be properly regularized. To this end, we use the results of [29], where the fermion-loop with bare propagators are discussed. It is found that the  $M_0$ -term in Eq. (80) is canceled by the regularization procedure. We adopt this prescription also here and explicitly set  $M_0 = 0$ . Within our approximation scheme, this then entails that also the lowest Landau level of  $Z_0$  is unaffected by unquenching and  $Z_\parallel$  is the only dressing function that is modified. The remaining equation for  $Z_\parallel$  is finite due to dimensional reduction and needs no further regularization.

## V. RESULTS FOR FULL QCD

Here we present results for the unquenched system of two up/down quarks back-coupled to the Yang-Mills sector in the above described approximation. To this end we need to take into account the different charges of the quarks. The magnetic background field then breaks the isospin

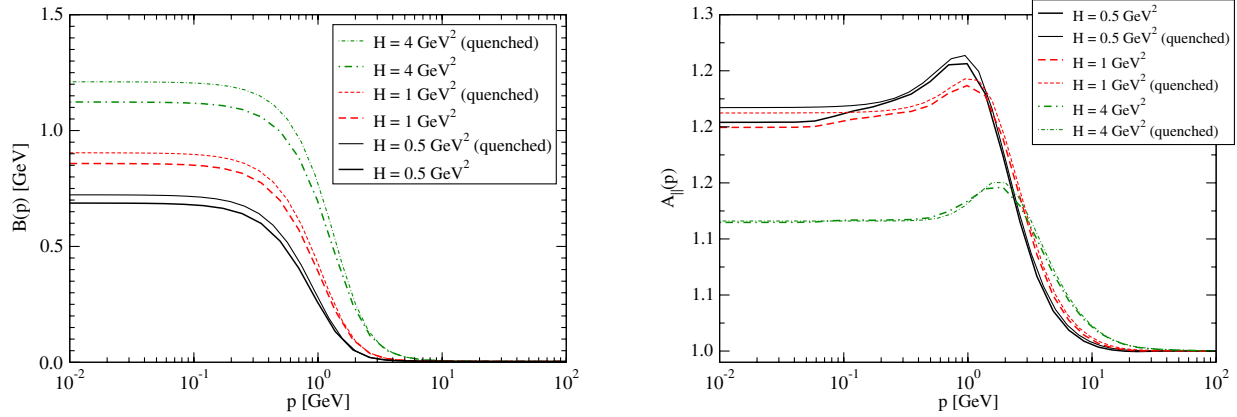


FIG. 7 (color online). Unquenched dressing functions  $B$  and  $A_{\parallel}$  of the up quark propagator (lowest Landau level) for different magnetic fields as a function of  $p \equiv p_{\parallel}$  at a bare quark mass of  $m = 3.7$  MeV at  $\mu = 100$  GeV. The dressing function  $A_{\perp}$  is not defined on the lowest Landau level.

symmetry of the system by coupling differently to the charges  $+2/3e$  of the up-quark and  $-1/3e$  of the down quark. We take this fully into account by solving for two quark DSEs for the up- and down-quark. Correspondingly, in Eqs. (78)–(80) we take into account one quark-loop for the up- and one for the down-quark with respective charges.

Let us first discuss the effects of the magnetic field in the Yang-Mills sector. The only nontrivial (i.e. unquenched) longitudinal part  $Z_{\parallel}(k_1, k_2, k_{\parallel})$  of the gluon dressing is displayed in Fig. 6 for different momentum slices along  $k_1 \equiv k_{\perp}^1$ ,  $k_2 \equiv k_{\perp}^2$  and  $k_{\parallel}$ . Overall, we find that the changes of the gluon propagator due to the magnetic field are very much dependent on the kinematics. For  $Z_{\parallel}(k_1, k_2)$  almost nothing happens, whereas unquenching effects are largest for the low- and mid-momentum behavior in  $Z_{\parallel}(k_1, k_{\parallel})$  and  $Z_{\parallel}(k_2, k_{\parallel})$ , where the typical ‘‘bump’’ in the gluon dressing function gets reduced by the presence of the quarks. In general, this reduction is typical for unquenched systems and has been observed for the case of zero magnetic field in lattice as well as Dyson-Schwinger studies (see e.g. [54,56–58]). For stronger magnetic fields with growing effects due to dynamical chiral symmetry breaking, this reduction gets ever stronger, notably in the  $k_1$  and  $k_2$  directions of the plots. In contrast, the  $k_{\parallel}$ -directions as well as the high ultraviolet behavior of the gluon dressing functions are hardly affected by the magnetic field.

The corresponding dressing functions for the quark propagator are shown in Fig. 7. We display the dressing functions  $B$  and  $A_{\parallel}$  for an up quark with charge  $q_f = +2/3e$  on the lowest Landau level as a function of momentum  $p_{\parallel}$  and compare with the corresponding quenched result. Note that  $A_{\perp}$  is not shown, since it is only defined for higher Landau levels. Also in the unquenched case we observe that the scalar dressing function  $B$  grows with larger magnetic field. However, this growth is less pronounced as in the quenched case. Clearly, the reduction of the gluon dressing function due to

the quark-loop leads to reduced interaction strength in the quark DSE as compared to the quenched case and this reduces the amount of chiral symmetry breaking. For  $A_{\parallel}$ , displayed on the right-hand side of Fig. 7, we find only small changes. Similar to the quenched case we find an increase in  $A_{\parallel}(0)$  as a function of magnetic field for smaller fields (not shown in the plot) with a maximum at  $|eH| = 0.5$  GeV<sup>2</sup>. As can be seen in Fig. 7, for larger fields,  $A_{\parallel}(0)$  decreases again, but the rate is considerably smaller than for the quenched case. For extremely large magnetic field we find that  $A_{\parallel}(0) \approx 1$ . This suggests that the different behavior found in Sec. III is particular to the quenched approximation.

Next we discuss the behavior of the quark condensate as a function of the external field as displayed in Fig. 8. Here, we observe the breaking of isospin symmetry due to the different charges of the up and down quarks, resulting in a different slope of the condensate as a function of  $eH$ . Similar to the quenched case we find a power law behavior of the condensate proportional to a linear term and a term

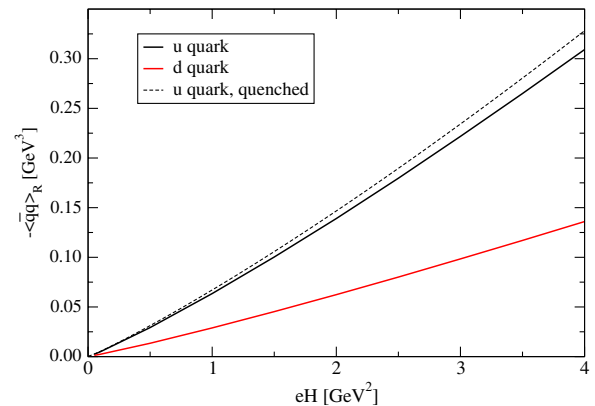


FIG. 8 (color online). Unquenched quark condensate for the up- and down-quark.

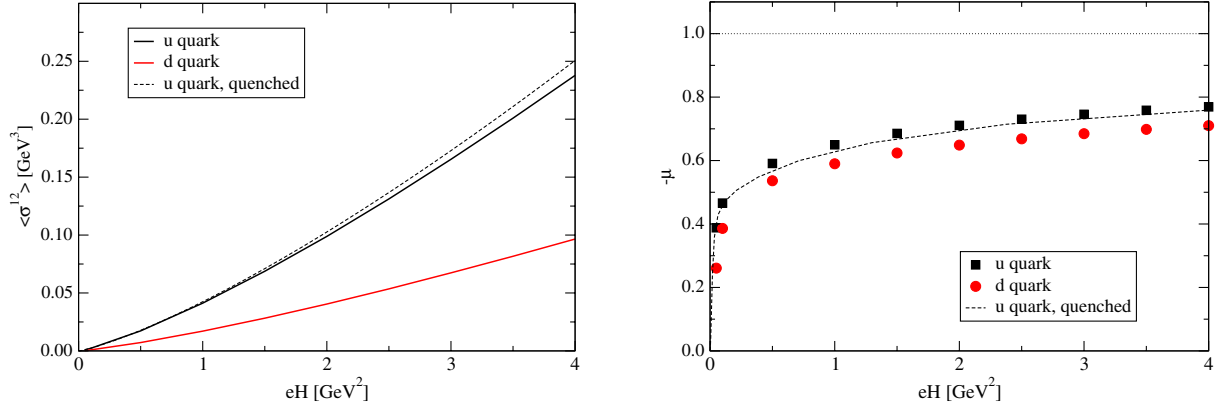


FIG. 9 (color online). Left: regularized expectation value of the spin polarization tensor  $\langle \sigma^{12} \rangle$ . Right: regularized magnetic polarization  $\mu$  of the QCD vacuum.

$\sim (eH)^{3/2}$  compatible with the expected behavior for the condensate for fields  $eH > m_\pi^2$  and at asymptotically large values of the field. The unquenching effects in the condensate are small but qualitatively significant. On the one hand, the amount of condensate generated is decreased in accord with our results for the scalar dressing function discussed above; the backreaction of the quarks onto the gluon leads to a *reduced amount of magnetic catalysis* as compared to the quenched case. This finding agrees with the results of Ref. [28]. On the other hand, the range of magnetic fields which are dominated by the linear behavior of the condensate is of the same order. Whereas for the quenched case, the  $(eH)^{3/2}$  term in the condensate becomes comparable in size with the linear one for fields around  $eH \sim 12$  GeV<sup>2</sup>, this happens in the unquenched case around  $eH \sim 14$  GeV<sup>2</sup>. The corresponding fits to the up-quark condensate of the form

$$\langle \bar{q}q \rangle \sim a_1 |eH| + a_2 |eH|^{3/2}, \quad (90)$$

are given by  $a_1 = 0.052$  GeV,  $a_2 = 0.015$  in the quenched case and  $a_1 = 0.0503$  GeV,  $a_2 = 0.0136$  for the unquenched case.

Similar effects as for the condensate can be observed for the expectation value of the spin polarization shown in the left diagram of Fig. 9. The unquenching effects are quantitatively similar as for the quark condensate. This can also be seen in the magnetic polarization of the vacuum, shown in the right diagram of Fig. 9. Since the unquenching effects in the condensate and spin polarization are almost similar, the ratio of the two is not drastically affected. Especially for large fields, the quenched results are very close to the unquenched one, whereas for small fields we observe unquenching corrections of the order of ten percent. Similar to the quenched case, the polarizability rises only slowly with magnetic field and approaches its asymptotic limit  $\mu \rightarrow 1$  only for extremely large fields.

## VI. SUMMARY AND CONCLUSIONS

In this work we studied the influence of (strong) magnetic fields onto the quark and gluon propagators of Landau gauge QCD and the associated quark condensate and spin polarization. Our most important observation is the *decrease in magnetic catalysis* induced by the backreaction of the quarks onto the Yang-Mills sector. We find a considerable reduction of the gluon dressing function  $Z_{\parallel}$  in the midmomentum region due to the magnetic field induced changes in the quark-loop of the gluon DSE. Compared to the quenched case, this reduces the interaction strength in the quark DSE and leads to a smaller amount of chiral symmetry breaking, reducing the corresponding order parameters, i.e. the scalar quark dressing function and the quark condensate. Unquenching effects in the gluon sector therefore contribute to *magnetic inhibition* in addition to the *magnetic catalysis* effects in the quark sector. This finding agrees with the interpretation of *inverse magnetic catalysis* due to magnetic effects on the gluonic background given in the context of recent lattice studies [13,16].

For the quenched and unquenched quark condensate, we find a linear dependence on the magnetic field for  $eH \geq \Lambda_{\text{QCD}}^2$ , which gradually develops additional components  $\sim (eH)^{3/2}$  for larger fields. This additional component becomes dominant only for extremely large magnetic fields indicating the asymptotic nature of this component.

Our framework takes into account also effects from higher Landau levels and therefore enables us to assess the validity of the LLL approximation. In general we observe sizable contributions from the higher Landau levels such that the LLL approximation, although valid on the ten percent level, becomes exact only at asymptotically large fields.

Finally, we would like to emphasize that unquenching effects due to the hadronic backreaction onto the system are not yet included in our truncation scheme. These effects would show up in the details of the quark-gluon vertex [59] which need to be resolved diagrammatically for that

purpose. In the model study of Ref. [22], effects from neutral mesons are found to reduce the amount of quark condensate generated and therefore contribute qualitatively similar to the *magnetic inhibition* of the system as the effects in the gluon sector discussed in this work. It remains to be seen in a more general study, how the unquenching effects in the gluon and meson sectors compare on a quantitative basis. Very recent results indeed suggest, that meson effects alone are not sufficient to explain inverse magnetic catalysis at finite temperature [60].

### ACKNOWLEDGEMENTS

C.F. thanks the Yukawa Institute for Theoretical Physics, Kyoto University, where this work was completed during the YITP-T-13-05 workshop on “New Frontiers in QCD.” This work was supported by the Helmholtz International Center for FAIR within the LOEWE program of the State of Hesse and the Studienstiftung des deutschen Volkes.

### GLUON PROPAGATOR AND QUARK-GLUON VERTEX

In this study we employ a truncation scheme for the quark-gluon vertex based on results found in [42] with some minor modifications. There, for the quenched gluon propagator, a fit to lattice data has been employed. It is given by

$$Z(k^2) = \frac{q^2 \Lambda^2}{(q^2 + \Lambda^2)^2} \left[ \left( \frac{c}{q^2 + a\Lambda^2} \right)^b + \frac{q^2}{\Lambda^2} \left( \frac{\beta_0 \alpha(\mu) \log q^2 / \Lambda^2 + 1}{4\pi} \right)^\gamma \right] \quad (\text{A1})$$

with the parameters

$$a = 0.60, \quad b = 1.36, \quad \Lambda = 1.4 \text{ GeV}, \quad (\text{A2})$$

$$c = 11.5 \text{ GeV}^2, \quad \beta_0 = 11N_c/3, \quad \gamma = -13/22, \quad (\text{A3})$$

where  $\alpha(\mu) = 0.3$ . Since the quenched gluon propagator does not get modified by the presence of an external magnetic field, this form is exact within the limits of the systematic error of the lattice data. In our calculations of the unquenched gluon propagator, this form acts as a seed which is supplemented by the quark-loop, see the main text for details.

For the quark-gluon vertex we use the approximation  $\Gamma^\nu \rightarrow \gamma^\nu \Gamma(k^2)$ . The vertex is then given in terms of the gluon momentum only, which in the Ritus case is still a “physical” momentum (in contrast to the Ritus eigenvalues). As explained in the main body of this manuscript [above Eq. (20)], such an ansatz is necessary to also make the integration over the second space-time coordinate analytically feasible and therefore decreases the required numerical effort to a manageable amount. More refined constructions may involve the Ward identity in the presence of magnetic fields [43] and therefore resemble the Ball-Chiu construction of the vertex in the corresponding case of zero magnetic field. Such constructions have been used to explicitly take into account the expected dependence of the vertex on external parameters such as temperature, chemical potential or the number of fermion flavors [42,44,61]. While these constructions led to quantitative improvements in the response of the system to changes in the external parameters, the qualitative behavior has not been affected<sup>1</sup>. Pending more refined studies we assume here that this is also the case for external magnetic fields.

For the vertex dressing function  $\Gamma(k^2)$  we use

$$\Gamma(k^2) = \frac{d_1}{d_2 + q^2} + \frac{q^2}{\Lambda^2 + q^2} \left( \frac{\beta_0 \alpha(\mu) \log q^2 / \Lambda^2 + 1}{4\pi} \right)^{2\delta}, \quad (\text{A4})$$

where  $k$  is the gluon momentum. The parameters used are

$$d_1 = 7.9 \text{ GeV}^2, \quad d_2 = 0.5 \text{ GeV}^2, \quad (\text{A5})$$

$$\delta = -18/88, \quad \Lambda = 1.4 \text{ GeV}. \quad (\text{A6})$$

The form of the ansatz is similar than in [42]. However, there the ansatz has been employed together with the first term of the Ball-Chiu form of the vertex. Here, we use it together with a bare vertex, which results in a change of the strength parameter  $d_1$ , which is  $d_1 = 7.9 \text{ GeV}^2$  instead of  $d_1 = 4.6 \text{ GeV}^2$  as in the reference. The other parameter  $d_2$  represents a scale, which is adjusted to the scale inherent in the lattice data for the gluon propagator and remains unchanged as compared with [42].

<sup>1</sup>This has been explicitly studied e.g. in Ref. [61] for the case of the chiral transition in strong QED<sub>3</sub> with respect to the number of fermion flavors. For this particular case it has even been found that the most refined dressings of the vertex led to a result close to the bare vertex, whereas less advanced truncations, such as the first term of a Ball-Chiu construction were further off.

- [1] I. A. Shovkovy, *Lect. Notes Phys.* **871**, 13 (2013).
- [2] R. Gatto and M. Ruggieri, *Lect. Notes Phys.* **871**, 87 (2013).
- [3] M. D’Elia, *Lect. Notes Phys.* **871**, 181 (2013).
- [4] K. Fukushima, *Lect. Notes Phys.* **871**, 241 (2013).
- [5] M. Frasca and M. Ruggieri, *Phys. Rev. D* **83**, 094024 (2011).
- [6] E. S. Fraga, B. W. Mintz, and J. Schaffner-Bielich, *Phys. Lett. B* **731**, 154 (2014).
- [7] T. Kojo and N. Su, *Phys. Lett. B* **720**, 192 (2013); T. Kojo and N. Su, *Phys. Lett. B* **726**, 839 (2013).
- [8] V. Skokov, *Phys. Rev. D* **85**, 034026 (2012).
- [9] K. Fukushima and J. M. Pawłowski, *Phys. Rev. D* **86**, 076013 (2012).
- [10] J. O. Andersen and A. Tranberg, *J. High Energy Phys.* **08** (2012) 002; J. O. Andersen, W. R. Naylor, and A. Tranberg, [arXiv:1311.2093](https://arxiv.org/abs/1311.2093).
- [11] M. D’Elia and F. Negro, *Phys. Rev. D* **83**, 114028 (2011).
- [12] C. Bonati, M. D’Elia, M. Mariti, F. Negro, and F. Sanfilippo, *Phys. Rev. D* **89**, 054506 (2014).
- [13] G. S. Bali, F. Bruckmann, G. Endrodi, Z. Fodor, S. D. Katz, and A. Schafer, *Phys. Rev. D* **86**, 071502 (2012).
- [14] G. S. Bali, F. Bruckmann, G. Endrodi, Z. Fodor, S. D. Katz, S. Krieg, A. Schafer, and K. K. Szabo, *J. High Energy Phys.* **02** (2012) 044.
- [15] G. S. Bali, F. Bruckmann, M. Constantinou, M. Costa, G. Endrodi, S. D. Katz, H. Panagopoulos, and A. Schafer, *Phys. Rev. D* **86**, 094512 (2012).
- [16] G. S. Bali, F. Bruckmann, G. Endrodi, F. Gruber, and A. Schaefer, *J. High Energy Phys.* **04** (2013) 130; F. Bruckmann, G. Endrodi, and T. G. Kovacs, *J. High Energy Phys.* **04** (2013) 112.
- [17] P. V. Buividovich, M. N. Chernodub, E. V. Luschevskaya, and M. I. Polikarpov, *Phys. Lett. B* **682**, 484 (2010).
- [18] V. V. Braguta, P. V. Buividovich, T. Kalaydzhyan, S. V. Kuznetsov, and M. I. Polikarpov, *Phys. At. Nucl.* **75**, 488 (2012).
- [19] E. -M. Ilgenfritz, M. Kalinowski, M. Muller-Preussker, B. Petersson, and A. Schreiber, *Phys. Rev. D* **85**, 114504 (2012).
- [20] E. -M. Ilgenfritz, M. Muller-Preussker, B. Petersson, and A. Schreiber, *Phys. Rev. D* **89**, 054512 (2014).
- [21] V. P. Gusynin, V. A. Miransky, and I. A. Shovkovy, *Nucl. Phys.* **B462**, 249 (1996).
- [22] K. Fukushima and Y. Hidaka, *Phys. Rev. Lett.* **110**, 031601 (2013).
- [23] M. N. Chernodub, *Phys. Rev. Lett.* **106**, 142003 (2011).
- [24] V. V. Braguta, P. V. Buividovich, M. N. Chernodub, A. Y. Kotov, and M. I. Polikarpov, *Phys. Lett. B* **718**, 667 (2012).
- [25] Y. Hidaka and A. Yamamoto, *Phys. Rev. D* **87**, 094502 (2013).
- [26] F. Bruckmann and G. Endrodi, *Phys. Rev. D* **84**, 074506 (2011).
- [27] D. S. Lee, C. N. Leung, and Y. J. Ng, *Phys. Rev. D* **55**, 6504 (1997).
- [28] V. A. Miransky and I. A. Shovkovy, *Phys. Rev. D* **66**, 045006 (2002).
- [29] C. N. Leung and S.-Y. Wang, *Ann. Phys. (Amsterdam)* **322**, 701 (2007); *Nucl. Phys.* **B747**, 266 (2006).
- [30] A. Ayala, A. Bashir, A. Raya, and E. Rojas, *Phys. Rev. D* **73**, 105009 (2006).
- [31] E. Rojas, A. Ayala, A. Bashir, and A. Raya, *Phys. Rev. D* **77**, 093004 (2008).
- [32] G. Murguía, A. Raya, A. Sanchez, and E. Reyes, *Am. J. Phys.* **78**, 700 (2010).
- [33] P. Watson and H. Reinhardt, *Phys. Rev. D* **89**, 045008 (2014).
- [34] V. I. Ritus, *Ann. Phys. (N.Y.)* **69**, 555 (1972); V. I. Ritus, *Zh. Eksp. Teor. Fiz.* **75**, 1560 (1978) [*V. I. Ritus Sov. Phys. JETP* **48**, 788 (1978)].
- [35] V. I. Ritus, in *Issues in Intense-Field Quantum Electrodynamics*, edited by V. L. Ginzburg (Nova Science Publishers, Unites States, 1987) p. 180.
- [36] D. Leinweber, J. Skullerud, A. Williams, and C. Parrinello (UKQCD Collaboration), *Phys. Rev. D* **60**, 094507 (1999); D. Leinweber, J. Skullerud, A. Williams, and C. Parrinello (UKQCD Collaboration), *Phys. Rev. D* **61**, 079901(E) (2000).
- [37] A. Cucchieri and T. Mendes, *Proc. Sci., LAT2007* (2007) 297 [[arXiv:0710.0412](https://arxiv.org/abs/0710.0412)].
- [38] I. L. Bogolubsky, E. M. Ilgenfritz, M. Muller-Preussker and A. Sternbeck, *Phys. Lett. B* **676**, 69 (2009); A. Sternbeck, E. M. Ilgenfritz, M. Muller-Preussker, A. Schiller, and I. L. Bogolubsky, *Proc. Sci., LAT2006* (2006) 076 [[arXiv:hep-lat/0610053](https://arxiv.org/abs/hep-lat/0610053)].
- [39] A. C. Aguilar, D. Binosi and J. Papavassiliou, *Phys. Rev. D* **78**, 025010 (2008); *Phys. Rev. D* **84**, 085026 (2011).
- [40] C. S. Fischer, A. Maas, and J. M. Pawłowski, *Ann. Phys. (Amsterdam)* **324**, 2408 (2009).
- [41] M. Q. Huber and L. von Smekal, *J. High Energy Phys.* **04** (2013) 149.
- [42] C. S. Fischer, A. Maas, and J. A. Muller, *Eur. Phys. J. C* **68**, 165 (2010).
- [43] E. J. Ferrer and V. de la Incera, *Phys. Rev. D* **58**, 065008 (1998).
- [44] C. S. Fischer and J. Luecker, *Phys. Lett. B* **718**, 1036 (2013).
- [45] T. D. Cohen, D. A. McGady, and E. S. Werbos, *Phys. Rev. C* **76**, 055201 (2007).
- [46] I. A. Shushpanov and A. V. Smilga, *Phys. Lett. B* **402**, 351 (1997).
- [47] L. von Smekal, K. Maltman, and A. Sternbeck, *Phys. Lett. B* **681**, 336 (2009).
- [48] B. L. Ioffe and A. V. Smilga, *Nucl. Phys.* **B232**, 109 (1984).
- [49] I. A. Batalin and A. E. Shabad, *Zh. Eksp. Teor. Fiz.* **60**, 894 (1971).
- [50] A. E. Shabad, *Ann. Phys. (N.Y.)* **90**, 166 (1975).
- [51] W. Dittrich and H. Gies, *Springer Tracts Mod. Phys.* **166**, 1 (2000).
- [52] W. H. Furry, *Phys. Rev.* **51**, 125 (1937).
- [53] K. Hattori and K. Itakura, *Ann. Phys. (Amsterdam)* **330**, 23 (2013).
- [54] C. S. Fischer and R. Alkofer, *Phys. Rev. D* **67**, 094020 (2003).

- [55] J. Luecker, Ph.D thesis, University of Giessen, Germany, 2013, [http://geb.uni-giessen.de/geb/volltexte/2013/10128/pdf/LueckerJan\\_2013\\_10\\_11.pdf](http://geb.uni-giessen.de/geb/volltexte/2013/10128/pdf/LueckerJan_2013_10_11.pdf); see Fig. 6.2. on page 42.
- [56] P. O. Bowman, U. M. Heller, D. B. Leinweber, M. B. Parappilly, and A. G. Williams, *Phys. Rev. D* **70**, 034509 (2004).
- [57] C. S. Fischer, P. Watson, and W. Cassing, *Phys. Rev. D* **72**, 094025 (2005).
- [58] A. C. Aguilar, D. Binosi, and J. Papavassiliou, *Phys. Rev. D* **88**, 074010 (2013).
- [59] C. S. Fischer, D. Nickel, and J. Wambach, *Phys. Rev. D* **76** (2007) 094009; C. S. Fischer and R. Williams, *Phys. Rev. D* **78**, 074006 (2008).
- [60] K. Kamikado and T. Kanazawa, *J. High Energy Phys.* 03 (2014) 009.
- [61] C. S. Fischer, R. Alkofer, T. Dahm, and P. Maris, *Phys. Rev. D* **70**, 073007 (2004).